Université catholique de Louvain

Institut de Statistique, Biostatistique et Actuariat

The impact of Covid-19 on the mortality of the Belgian population .

Membres du jury:

Prof. Donatien Hainaut, *Promoteur*
Julien Antunes Mendes, *Co-Promoteur*
Prof. Jérôme Barbarin, *Lecteur*

Mémoire présenté en vue de
l'obtention du master
en sciences actuarielles
(orientation sciences actuarielles)
par:

Cédric Turcksin

Louvain-La-Neuve
Janvier 2022

Preface.

This dissertation has been prepared in partial fulfillment of the requirements for the master degree in actuarial sciences delivered by the Université Catholique de Louvain.
This dissertation is the result of an internship carried out during the year 2020 at Reacfin in the Centre of Excellence Life, Health & Pension.

Acknowledgment.

First of all, I would like to thank the whole Reacfin team who welcomed me during this particular period. Their friendliness and their availability allowed me to carry out a part of this dissertation in complete serenity as well as to discover a united team with fun and original activities.

I would also like to thank the Reacfin Centre of Excellence Life, Health & Pension where I was integrated without any difficulty and especially my training supervisor Julien Antunes Mendes who guided me throughout this work with his good mood and humour.

Finally, I would like to thank the School of Statistics, Biostatistics and Actuarial Sciences of the Catholic University of Louvain, who accepted my internship and in particular Donatien Hainaut who accepted to be my promoter. His support has been essential for the successful completion of this work.

Contents

Chapter 1

Introduction.

The coronavirus crisis, called Covid-19, started in November 2019 in Wuhan, Republic of China. Shortly afterwards, the virus spread rapidly around the world and reached Belgium in February 2020. The number of deaths caused by this pandemic for 2020 is estimated to be around 20 000 deaths in Belgium. Most of the deaths are due to two waves that occurred in Belgium and in the rest of Europe. In more detail, the total number of deaths in 2020 was equal to 126 850 for the Belgian population. For comparison, in 2019 it was 108 745. Moreover, the pandemic was not the only major event that occurred in the year 2020. Indeed, the lockdown that was put in place to deal with this pandemic also had his impact on the mortality of Belgian population. The aim of this dissertation is precisely to study the impact of Covid-19 and the lockdown on the mortality of the Belgian population for the year 2020.

More specifically, we will see how Covid-19 influences the calibration of a stochastic mortality model such as the Lee-Carter. We will also discuss the effect of the pandemic on the projection method used and how we can use this event to incorporate future pandemics into the projection method. We will use a total of 6 different projection methods such as the basic random walk scheme with drift, a method we will call "deformation of the curve" and finally we will use a projection method with permanent and transitory jump effects with two different distributions for the jumps. For all these projection models, we will also discuss the advantages and disadvantages of each method and the effect that the projection method has on future life expectancies and future life annuities.

In the last chapter, we will also see how some of the projection methods developed in this dissertation behave under a different mortality model. Indeed, we will use a multi-population model to assess the impact of Covid-19 and we will see the differences between this model and the Lee-Carter model.

Chapter 2

Notation & Data.

2.1 Notation.

Throughout this work, we will use certain notations which are detailed below.
Let us assume that :

- $D_{x,t}$ is the number of deaths recorder at age x in year t.
- $ETR_{x,t}$ is the exposure to risk or risk exposure that corresponds to the total time lived by people aged x at the last birthday in calendar year t.
- $\mu_{x,t}$ is the mortality rate. Intuitively, we can see $\mu_{x,t}$ as a measure of the risk for an individual aged x in year t to die instantly.
- $p_{x,t}$ is the probability of surviving to age $x+1$ for year t.
- $q_{x,t}$ is the probability of dying before age $x+1$ for year t.

Observed mortality rates can be obtained by dividing the number of deaths $D_{x,t}$ recorded at age x in year t by the corresponding risk exposure $ETR_{x,t}$:

$$\mu_{x,t} = \frac{D_{x,t}}{ETR_{x,t}}. \tag{2.1.1}$$

We also make the traditional assumption that $\mu_{x,t}$ is piecewise constant :

$$\mu_{x+s,t+s} = \mu_{x,t} \quad \text{for } 0 \leq s < 1. \tag{2.1.2}$$

By using (2.1.2), we can link $p_{x,t}$ and $q_{x,t}$ with $\mu_{x,t}$ by noting that :

$$p_{x,t} = \exp(-\mu_{x,t}) \tag{2.1.3}$$
$$q_{x,t} = 1 - p_{x,t} \tag{2.1.4}$$

The probability of surviving to age $x+s$ knowing that we are alive at age x for year t, denoted ${}_sp_{x,t}$ afterwards, can be written as :

$$\begin{aligned} {}_sp_{x,t} &= p_{x,t} \times_{s-1} p_{x+1,t} \\ &= p_{x,t} \times p_{x+1,t} \times \ldots \times p_{x+s-1,t}. \end{aligned} \tag{2.1.5}$$

Intuitively, the probability of surviving till time s, is the product of yearly survival probabilities from age x to $x+s$.

2.2 Data.

All stochastic mortality and predictive models are calibrated using data from the human mortality database HMD [1]. In this database, we use the tables "Deaths" and "Exposure to risk" in 1x1 format for the Belgian population to perform the calibration of our mortality models. We use as age range $x = \{0, \ldots, 99\}$ and as period range $t = \{1980, \ldots, 2020\}$.

The choice of this age range and period range is justified by the fact that we want to evaluate the impact of Covid-19 on the Belgian population. Fortunately or unfortunately for us, Covid-19 affected more severely the 85+ age group, which obliges us to take an age group up to 99. We do not use data above 99 because at a very old age, data become too volatile to be use with confidence.

In Figure 2.2.1, we show for the Belgian population (i.e. men + women) the number of deaths per age and the risk exposure for the year 2020 compared with the average observed for the period $2010 \rightarrow 2019$. We can clearly observe the effect of Covid-19 on the number of deaths $D_{x,t}$ for $x > 60$. Below this age, it is really difficult to see any real impact. Concerning the risk exposures for the year 2020, it was impacted by the combination of two distinct effects in addition to the normal evolution of the risk exposure. The first is obviously the increase of the number of deaths and the second is related to the effect of the lockdown on the movement of people in and out of Belgium.

[1] The mortality database is available at http://www.mortality.org

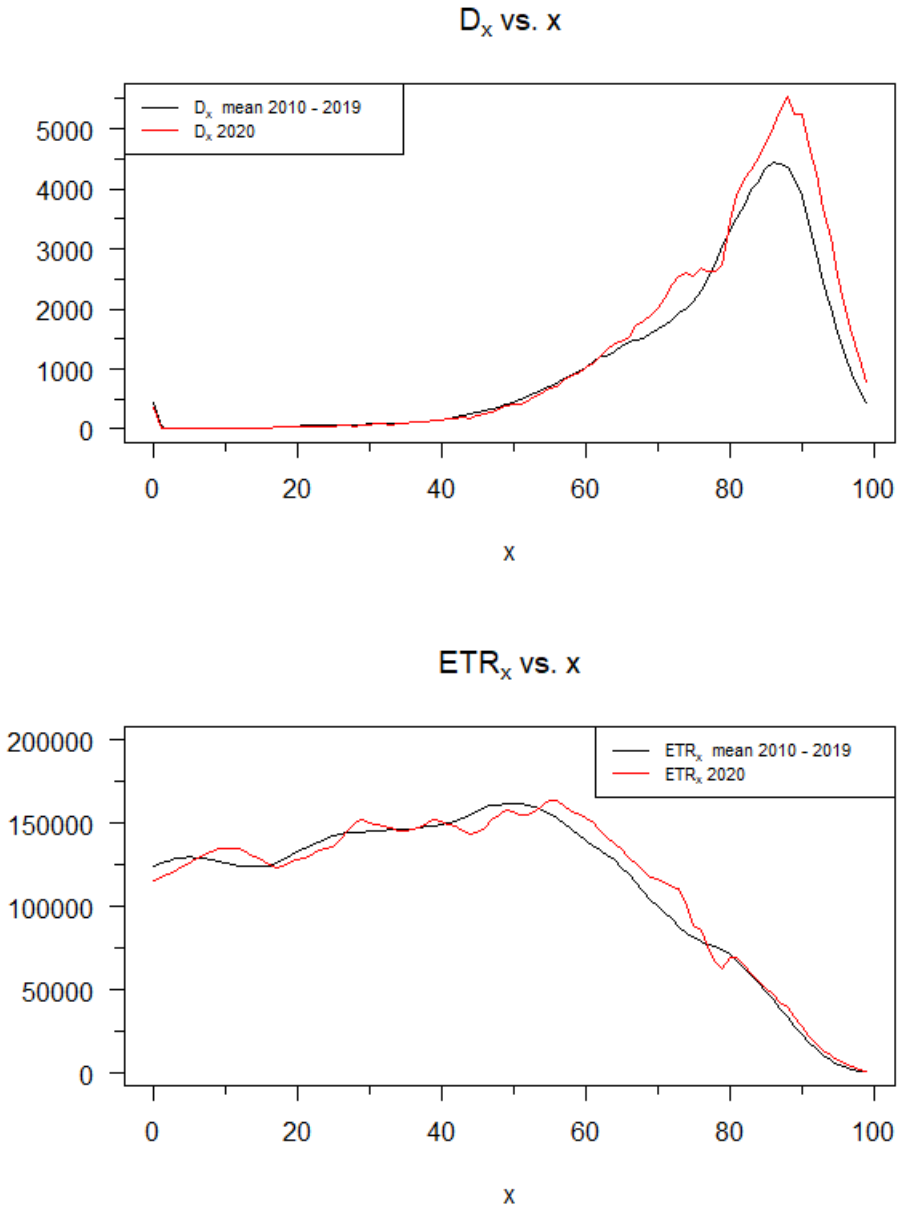

Figure 2.2.1: Number of deaths and risk exposure for the Belgian population. In red the year 2020 and in black the average observed for the period 2010 → 2019.

Chapter 3

Lee-Carter model (Theoretical aspect & Calibration).

3.1 Theoretical aspect.

One of the most popular stochastic mortality model is the one proposed by Lee and Carter (1992) [7]. This model decomposes mortality rates into 3 factors with one of them that can be seen as a time series to produce mortality projection. One of the great features of the Lee Carter model is its simplicity in describing the development of mortality rates for different ages. In fact, the model is given by :

$$\ln \mu_{x,t} = \alpha_x + \beta_x \kappa_t \tag{3.1.1}$$

where x represents the age and t the year.
The different parameters can be interpreted as follows :

- $\exp \alpha_x$ is the general shape (average level) of the mortality schedule at age x over time t.
- κ_t represents the time trend, i.e. the expected evolution of the mortality over time. We also call this term the mortality factor.
- β_x indicates the sensitivity of the logarithm of the force of mortality at age x to variations in the time index κ_t.

When we work with the Lee-Carter model, we need to impose a set of constraints on the parameters to ensure that the model is identifiable. Indeed, the parametrisation, regardless of how it is estimated, is not unique as illustrated below :

$$\ln \mu_{x,t} = \alpha_x + \frac{\beta_x}{c} \kappa_t \, c. \tag{3.1.2}$$

We can observe that for different values of c, we have an infinitive number of possible solutions for this equation. The following set of constraints on the parameters is generally accepted in the literature to avoid this problem and make the model identifiable :

$$\begin{cases} \sum_x \beta_x = 1 \\ \sum_t \kappa_t = 0 \end{cases} \tag{3.1.3}$$

Concerning the calibration, we can perform it under a Poisson setting. Brouhns et al. (2002) [1] implemented the Lee-Carter model assuming a Poisson distribution for the number of deaths as shown below :

$$D_{x,t} \sim \mathcal{P}\text{oisson}\big(ETR_{x,t}\,\mu_{x,t}\big). \tag{3.1.4}$$

The modelling of $D_{x,t}$ as a $\mathcal{P}$oisson variable can be considered intuitive as the number of deaths is a positive discrete value and a $\mathcal{P}$oisson distribution is well suited to mortality analyses. The parameters are estimated using the maximum likelihood estimation (MLE) and the log-likelihood function is given by :

$$\mathcal{L}(\theta) = \sum_{x,t} \Big(D_{x,t} \ln\big(ETR_{x,t}\,\mu_{x,t}(\theta)\big) - ETR_{x,t}\,\mu_{x,t}(\theta) - \ln\big(D_{x,t}!\big) \Big) \tag{3.1.5}$$

where θ are the parameters to be optimise.
The maximization of the log-likelihood is usually performed by a Newton-Raphson iterative procedure. Nevertheless, as pointed out by Currie (2016) [5], many stochastic mortality models, including the Lee-Carter model, can be considered as generalized linear models or generalized non-linear models. Therefore, standard statistical software[1] can be used to facilitate the fitting of these models. This is the procedure we choose to follow by using the R-package **StMoMo**[2] (Villegas et al. (2018) [10]). More specifically, we use the logarithm as link function and the function $fit(.)$ from the package to perform the calibration.

3.2 Calibration.

For the calibration, we take as time period and age group :

- ☐ $1980 \rightarrow 2020$
- ☐ $0 \rightarrow 99$

The calibration is performed using data for the entire Belgian population (men + women) and the parameters found by the calibration are displayed in Figure 3.2.1.

[1] We think at the standard function $glm(.)$ or $gnm(.)$ present in the package **gnm** (Turner and Firth (2020) [9]).
[2] StMoMo stands for Stochastic Mortality Modeling.

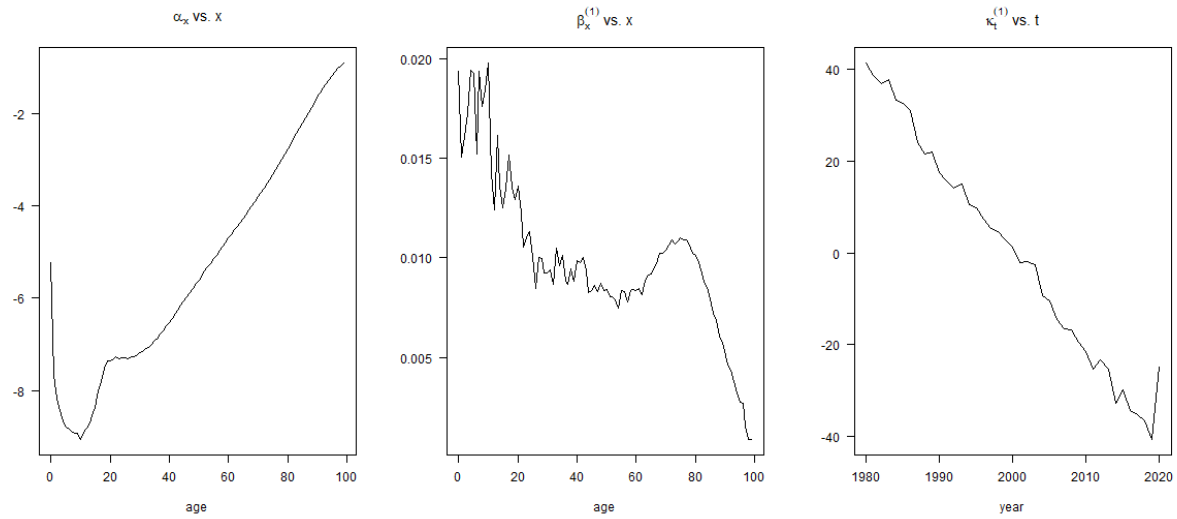

Figure 3.2.1: Calibration of the Lee-Carter model for the Belgian population.

We can clearly see the impact of Covid-19 on the mortality factor κ_t. For the period $1980 \rightarrow 2019$, we have a steady decrease in κ_t and consequently a decrease in mortality rates $\mu_{x,t}$. For 2020, we have a severe jump in the time series that leads to an increase in mortality rates. However, the severity of this jump depends on the age group considered. In fact, we put in Appendix A different calibrations where we have divided the age group into five different subgroups. This allow us to observe that the age group considering in the calibration has a big impact on the value of the jump observed in 2020. Indeed, for the youngest subgroup, the impact on the κ_t is very weak or even non-existent, whereas for the oldest subgroup, the impact is much stronger and more severe.

An important remark is that the Lee-Carter model is not the only stochastic mortality model that we can use. In fact, many different models can be used to perform mortality assessment. In the **StMoMo** package, we can easily fit other models such as CBD, APC, Plat, and many more. It would be interesting to see how these models behave with Covid-19 and how a particular mortality model performs across different countries. These questions cannot be answered here as it would take too much time but an R-shiny application has been developed to answer such questions. If anyone is interested, they are advised to consult Appendix B where they will find some information about the application and how to use it effectively.

In the following chapters we will discus the different ways to take into account the Covid-19 and future pandemics in a projection model. But first, we will study the case where we use a basic projection scheme and the change the year 2020 may have on the projection and the quality of the fit.

Chapter 4

Basic projection method.

4.1 Calibration.

One of the main topics of discussion regarding Covid-19 is the impact it might have on future mortality. At the moment, we still do not have a clear answer to this question, although we need to make mortality projections for the medium/long term especially for insurance purposes. Therefore, we need to assess the impact that Covid-19 may have on projection methods by making two projections with two different time periods for the calibration. One will take the year 2020 and the other will not, i.e.

- ☐ 1980 $\rightarrow$ 2019
- ☐ 1980 $\rightarrow$ 2020

Performing two simulations will allow us to clearly see the impact of Covid-19 on the projection method and more specifically, on the parameters composing the projection method. The first projection method that we use is the standard random walk with drift (**RWD**) discussed in Cairns et al. (2006) [2] and Haberman and Renshaw (2011) [6]. This method is defined as the reference and will be our point of comparison with the models detailed in the following chapters.

With the standard random walk with drift, the dynamics of the mortality factor κ_t can be described as follows :

$$\kappa_{t+1} = \kappa_t + \mu + \sigma Z_{t+1} \tag{4.1.1}$$

where μ and σ are constants, and $Z_{t+1} \sim \mathcal{N}(0, 1)$.
The calibration of the time series in (4.1.1) is performed by maximising the log-likelihood function.

Proposition 4.1.1. *Let us consider the following time series :*

$$z_t = \mu + \sigma Z_{t+1}.$$

The log-likelihood function of this model is then given by :

$$\ln f(z_1, \ldots, z_{K-1}) = \sum_{i=1}^{K-1} ln \left[\frac{1}{\sqrt{2\pi}\sigma} \exp \left(- \frac{(z_i - \mu)^2}{2\sigma^2} \right) \right].$$

Proof: By posing $z_t = \kappa_{t+1} - \kappa_t$, the equation (4.1.1) can be rewritten as :

$$z_t = \mu + \sigma Z_{t+1}.$$

We can observe that the variable z_t is normally distributed with mean μ and variance σ^2. Therefore, the density function of z_t, denoted by $f(z_t)$, is given by :

$$f(z_t) = \frac{1}{\sqrt{2\pi}\sigma} \exp \left(- \frac{(z_t - \mu)^2}{2\sigma^2} \right).$$

Note that if we have K observations for κ_t, there will be $K - 1$ observations for z_t. Eventually, the log-likelihood function is then given by :

$$\ln f(z_1, \ldots, z_{k-1}) = \sum_{i=1}^{K-1} \ln f(z_i)$$

which leads to the result.

□

By using the two time period defined above and the proposition 4.1.1, we can find the optimal parameters for the basic projection method (see Table 4.1.1).
By looking at the result, we can clearly see that placing the year 2020 in the calibration time period leads to an increase in the value of the parameters μ and σ. The increase is about 20% for μ and 57% for σ compared to the value these parameters have when we remove the year 2020. An increase in the value of μ means that mortality rates $\mu_{x,t}$ will decrease at a slower rate than before and an increase in the value of σ indicates that the uncertainty associated with κ_t and therefore $\mu_{x,t}$ is greater as illustrated in Figure 4.1.1.
Overall, we can see that with the basic projection method (i.e, a random walk with drift), the year 2020 has a tendency of increasing σ and strongly influence the mean value μ.

Another problem with this method is that the model does not allow future jumps that could be caused by future pandemics. Covid-19 proves that global pandemics are still a potential event that can occur at any time. This statement implies that jumps in the mortality factor can occur and working with a projection model that does not take this fact into account may be a mistake. Furthermore, pandemics are not the only events that can cause jumps in the mortality factor or mortality rates. Events such as earthquakes, tsunamis or events more related with Belgium, flooding and storm, can cause an excess of mortality for the year. The frequency and severity of these events may change rapidly due to climate change. For this reason, it is worth exploring projection models that take jumps into account, which will be developed in the following chapters.

Let us return to the basic model. In order to evaluate the quality of the fit and to be able to compare different models, we introduce the Akaike information criterion (AIC) and the Bayesian information criterion (BIC). The lower the AIC or BIC of the model, the better the quality of the fit will be.
The AIC can be defined as follows :

$$AIC = 2k - 2\ln\mathcal{L} \tag{4.1.2}$$

where k is the number of parameters to be estimate and $\mathcal{L}$ is the maximum likelihood function of the model.
The Bayesian information criterion (BIC) can be defined as follows :

$$BIC = -2\ln\mathcal{L} + k\ln N \tag{4.1.3}$$

where k is the number of parameters to be estimate, $\mathcal{L}$ is the maximum likelihood function of the model and N is the number of observations in the sample.
See bottom of Table 4.1.1 for the values for the basic projection method.

Time period	μ	σ
$1980 \rightarrow 2019$	-2.0738	2.2414
$1980 \rightarrow 2020$	-1.6605	3.5174

Time period	AIC	BIC
$1980 \rightarrow 2019$	177.64	180.97
$1980 \rightarrow 2020$	218.13	221.51

Table 4.1.1: Optimal parameters, AIC and BIC for the basic projection method.

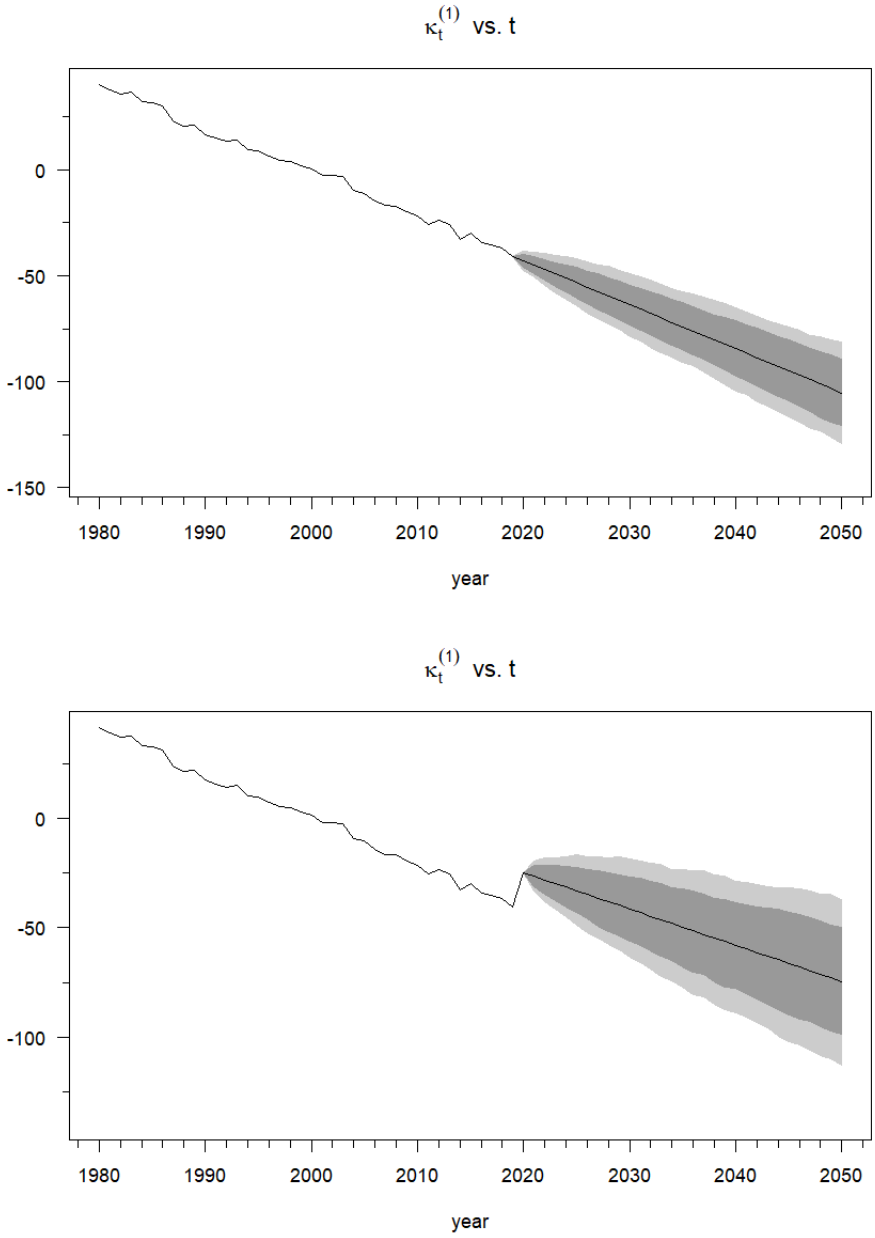

Figure 4.1.1: Projection of the mortality factor κ_t. the CI is set at 80% (dark grey) and 95% (light grey) .The first graph uses the time period 1980 $\rightarrow$ 2019 for the calibration and the second uses 1980 $\rightarrow$ 2020.

4.2 Life expectancy and life annuity.

With the optimal parameters found in the previous section, we can simulate future mortality rates $\mu_{x,t}$ by performing a Monte-Carlo simulation. For this dissertation, we limit the number of simulations to 1 000 and the maximum year of forecast is set to 2050. However, we still use the two calibration time periods defined above and thus have a total of two simulations. One with the year 2020 and one without.

With the two simulations, we are able to see the evolution over the year of life expectancies and the price of a life annuity. The life expectancies are calculated vertically, which means that the life expectancies for a particular year n are calculated by taking only the mortality rates for that particular year n. It is possible to show the following proposition.

Proposition 4.2.1. *Under the assumption that $\mu_{x+s,t+s}$ for $0 \leq s \leq 1$ is piecewise constant, then the life expectancy, denoted $e_{x,t}$, for age x and year t can be approached by :*

$$e_{x,t} = \sum_{s=1}^{w-x} {}_sp_{x,t}$$

where ${}_sp_{x,t}$ means the probability of surviving until age $x+s$ knowing that we are alive at age x for the year t and w is the maximum age reachable.

For our case, we set $w = 99$[1] and ${}_sp_{x,t}$ are calculated using equation (2.1.5). Life expectancies for different ages and years are shown in Table 4.2.1. This table contains the central forecast as well as the confidence interval at 95%.
If we take as an example the life expectancy of a person aged 20 for the year 2020, we see that this person loses approximately 1 year of life time because of Covid-19. In 2050, the gap is increase to 2 years between the two simulations.

For the life annuity, we have the following proposition.

Proposition 4.2.2. *Let us consider the payment of 1 € each year and starting at age x as long as the beneficiary lives and for $n - x$ years. The single net premium, noted $PU_{x,t}$ is equal to :*

$$PU_{x,t} = \sum_{i=0}^{n-x} {}_ip_{x,t}\, V^i$$

where $V = (1+r)^{-1}$ is the discount factor and t designed the year when the premium is computed.

[1] Clearly, 99 is not the maximum attainable age for a human being, but as we have limited ourselves to 99 for the calibration phase, we cannot go any further. It is possible to use a closure model to extend this limit but it is not studied here.

For both simulations, we take the example of a person aged 65 who will receive a life annuity until he reaches 99. Therefore, we set $x = 65$ and $n = 99$. We set the interest rate to 2% (see Table 4.2.2 for the results). As for life expectancies, we calculate the single premium for different years and the central forecast along with the confidence interval at 95% are put in the table.

We see that taking Covid-19 into account leads to a decrease of the single premium for a life annuity and an increase of the standard deviation. However, it should be mentioned that we have assumed that the interest rate is not affected by the Covid-19 crisis. We know that this assumption is not really true and that the decrease in price can be cancelled out by a decrease in the interest rate.

In the next chapter, we will study how to incorporate jumps and future pandemics to the basic projection method and the impact it may have on future life expectancies and future life annuities.

Calibration time period: 1980 → 2019

Age	2020	2030	2040	2050
20	**61.84** [61.48 ; 62.19]	**63.48** [62.29 ; 64.56]	**65.00** [63.55 ; 66.35]	**66.37** [64.67 ; 67.93]
40	**42.41** [42.07 ; 42.74]	**43.97** [42.84 ; 44.99]	**45.41** [44.03 ; 46.69]	**46.72** [45.09 ; 48.21]
60	**24.19** [23.89 ; 24.47]	**25.53** [24.55 ; 26.42]	**26.78** [25.59 ; 27.90]	**27.92** [26.51 ; 29.22]
80	**8.93** [8.78 ; 9.08]	**9.63** [9.12 ; 10.11]	**10.30** [9.66 ; 10.92]	**10.94** [10.15 ; 11.68]

Calibration time period: 1980 → 2020

Age	2020	2030	2040	2050
20	**60.71**	**61.79** [60.08 ; 63.47]	**63.10** [60.59 ; 65.46]	**64.33** [61.35 ; 66.76]
40	**41.23**	**42.36** [40.75 ; 43.94]	**43.60** [41.23 ; 45.84]	**44.76** [41.94 ; 47.07]
60	**22.90**	**24.13** [22.74 ; 25.49]	**25.19** [23.15 ; 27.13]	**26.20** [23.76 ; 28.20]
80	**8.15**	**8.89** [8.19 ; 9.59]	**9.44** [8.39 ; 10.47]	**9.97** [8.70 ; 11.07]

Table 4.2.1: Life expectancies calculated using the basic model. For the calibration time period 1980 → 2020, life expectancies for the year 2020 are calculated using mortality rates observed during the year.

Calibration time period: 1980 → 2019

Year	Single premium
2020	**16.22** [16.03 ; 16.40]
2030	**17.07** [16.45 ; 17.63]
2040	**17.85** [17.11 ; 18.55]
2050	**18.56** [17.69 ; 19.36]

Calibration time period: 1980 → 2020

Year	Single premium
2020	**15.35**
2030	**16.18** [15.28 ; 17.04]
2040	**16.85** [15.55 ; 18.07]
2050	**17.48** [15.95 ; 18.73]

Table 4.2.2: Single premium for a life annuity calculated using the basic model. For the calibration time period 1980 → 2020, single premiums for the year 2020 are calculated using mortality rates observed during the year.

Chapter 5

Introduction of jumps in the basic projection method.

5.1 Theoretical aspect.

In this chapter we study the case where we introduce mortality jumps without changing the dynamics of the basic projection method (i.e. a random walk with drift). The idea is to add a process on the mortality rates that we call a "deformation of the curve" to produce mortality jumps/shocks. The aim here is not to produce jumps in the mortality factor κ_t but rather to add a new process after the projection has been made using the standard projection method. As a reminder, the Lee-Carter model allows us to express mortality rates as :

$$\ln \mu_{x,t} = \alpha_x + \beta_x \kappa_t \tag{5.1.1}$$

and the mortality factor κ_t can be projected with :

$$\kappa_t = \kappa_t + \mu + \sigma Z_{t+1}. \tag{5.1.2}$$

If a pandemic or mortality shock occurs in year t', we introduce a process that causes mortality rates for that particular year to increase :

$$\hat{\mu}_{x,t'} = \mu_{x,t} \times \theta_x \tag{5.1.3}$$

where θ_x is the deformation of the curve. This process depends on x because excess of mortality caused by pandemics or other events can potentially have a different impact at different ages. This is the case for Covid-19 as illustrated in Appendix A.
If no mortality shock occurs in year t', then we have :

$$\hat{\mu}_{x,t'} = \mu_{x,t} \tag{5.1.4}$$

By combining the 3 equations above, we obtain a new dynamic for mortality rates :

$$\hat{\mu}_{x,t} = \exp\Big(\alpha_x + \beta_x \kappa_t\Big) \times \theta_x N_t \tag{5.1.5}$$

where N_t denotes the number of jumps occurring in year t. For simplicity, we assume that there is at most one jump event per year. N is then identically independently distributed and follows a binomial distribution with parameter p, i.e,

$$N = \begin{cases} 1 & \text{with probability } p \\ 0 & \text{with probability } 1-p \end{cases} \tag{5.1.6}$$

The parameter p can be interpreted as the probability that a pandemics occurs during the year. Provided an estimate of this parameter can be somewhat difficult as the occurrence of a pandemics is quite rare. Nevertheless, if we look at the last century, two majors pandemics occurred during this period: The Spanish flu ($1918 \rightarrow 1920$) and Covid-19. Other pandemics have occurred in the world during this century but not to the same extent as these two. For this reason, we choose to set the probability of occurrence at 2%, although other values can be possible[1].

5.2 Calibration of the deformation of the curve θ_x.

As our main goal is to analyse the impact of Covid-19 on mortality, we use this event to propose a form for the process θ_x. As a reminder, θ_x causes an excess of mortality for a particular year. Therefore, if we want to use the Covid-19 to calibrate this process, we need to extract the excess of mortality from the observed mortality rates in 2020. An approach to do this is simply by calibrate a Lee-Carter for the period $1980 \rightarrow 2019$ and project it one year ahead with a random walk with drift. As a result, we will have theoretical mortality rates for the year 2020 without the influence of Covid-19. The process θ_x is then the ratio between the two, i.e.

$$\theta_x = \frac{\mu_{x,2020}(\text{observed})}{\mu_{x,2020}(\text{theoretical})}. \tag{5.2.1}$$

The theoretical and observed logarithmic mortality rates for the year 2020 are represented in Figure 5.2.1. In Figure 5.2.2, we show the process θ_x obtained with (5.2.1).

[1]We will also study the case where we consider $p = 10\%$ to see the difference between the two.

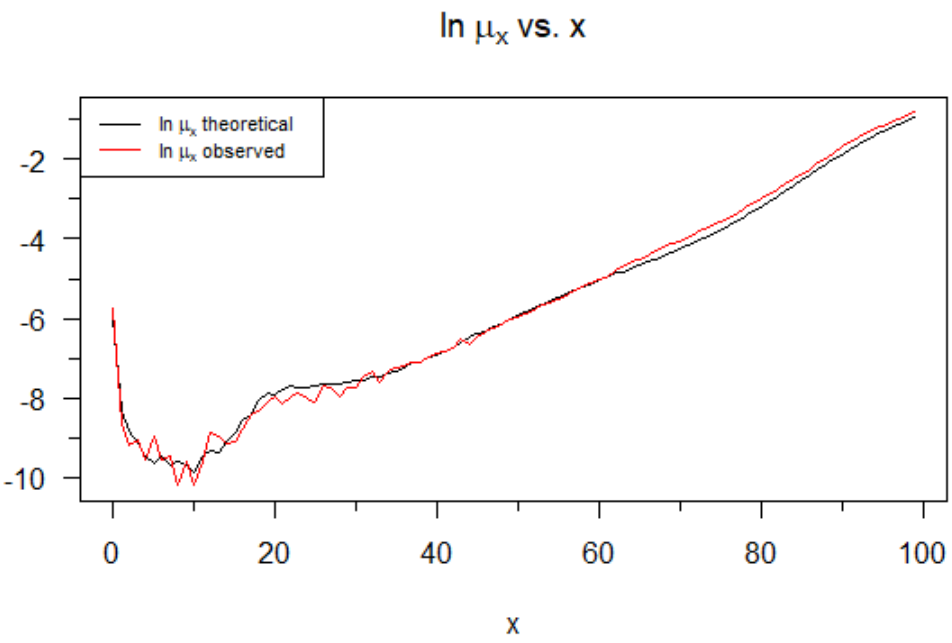

Figure 5.2.1: $\ln \mu_{x,2020}$(observed) in red and $\ln \mu_{x,2020}$(theoretical) in black for the Belgian population.

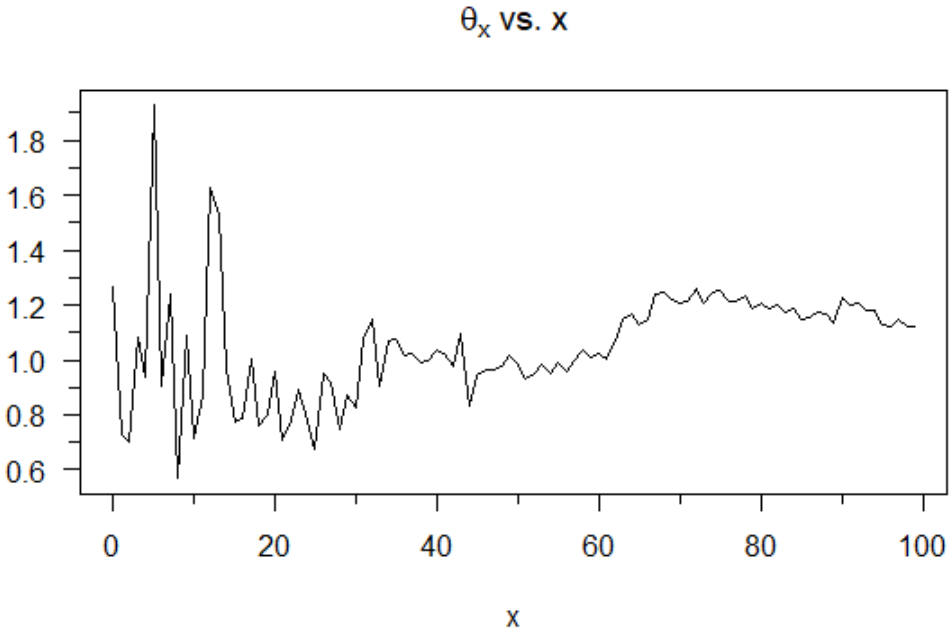

Figure 5.2.2: The process θ_x for the Belgian population.

Two observation can be made from Figure 5.2.1 . One is that we clearly see the excess of mortality created by Covid-19 for people over 60 and the other is to observe that we have a reduction in mortality for the age group $20 \rightarrow 30$ most likely created by the lockdown.

In the Figure 5.2.2, we can observe that the process θ_x shows some volatility, especially for the under-20s. As your main objective is to find the trend and not to reproduce exactly the effect of Covid-19, we can smooth the theoretical and observed mortality rates for 2020 by the Whittaker-Henderson method. In addition, we remove the effect on the youngest by setting $\theta_x = 1$ for $x < 18$.

The Whittaker-Henderson method can be considered as a non-parametric smoothing method based on two assumptions :

- the true curve μ_x should be close to it estimator $\hat{\mu}_x$.
- The curve μ_x should be smooth since the mortality increase with the age.

The quality of the fit can then be defined as :

$$F(c) = \sum_x w_x (c_x - \hat{\mu}_x)^2 \tag{5.2.2}$$

where F measures the distance between the curve c_x and $\hat{\mu}_x$. The sequence of weights w_x is a priori chosen.
The smoothness of a continuous curve can be assessed by its first and second order derivatives. In the discrete approximation, we use the difference operator Δ :

$$(\Delta c)_x = c_{x+1} - c_x. \tag{5.2.3}$$

Higher order differences can be defined iteratively :

$$(\Delta^z c) = \Delta(\Delta^{z-1} c). \tag{5.2.4}$$

The smoothness of the curve can then be measured by :

$$S(c) = \sum_x ((\Delta^z c)_x)^2. \tag{5.2.5}$$

The curve minimising $F(c)$ is $\hat{\mu}_x$ but this curve will not be smooth enough because $S(\hat{\mu})$ will be large. However, a polynomial curve of order z will minimize the quantity $S(c)$, but it will be too far from the raw curve $\hat{\mu}_x$. Therefore, we see that the curve c_x must be a compromise between these two quantities.

The Whittaker-Henderson method consists in finding this compromise by finding the curve c_x which minimises the quantity $\mathrm{WH}_h(c)$:

$$\mathrm{WH}_h(c) = F(c) + h\,S(c) \tag{5.2.6}$$

where h is a smoothing parameter that allows to tune the importance of smoothness in the global criterion.
When $h \longrightarrow 0$, $c_x \longrightarrow \hat{\mu}_x$ and if $h \longrightarrow +\infty$, c_x tends to a polynomial curve of order z.
For our case, we obtain good results by taking $w_x = ETR_x$, $h = 5$ and $z = 2$.

The process θ_x obtained using the theoretical and observed mortality rates smoothed by the Whittaker-Henderson method describe above is shown in Figure 5.2.3.

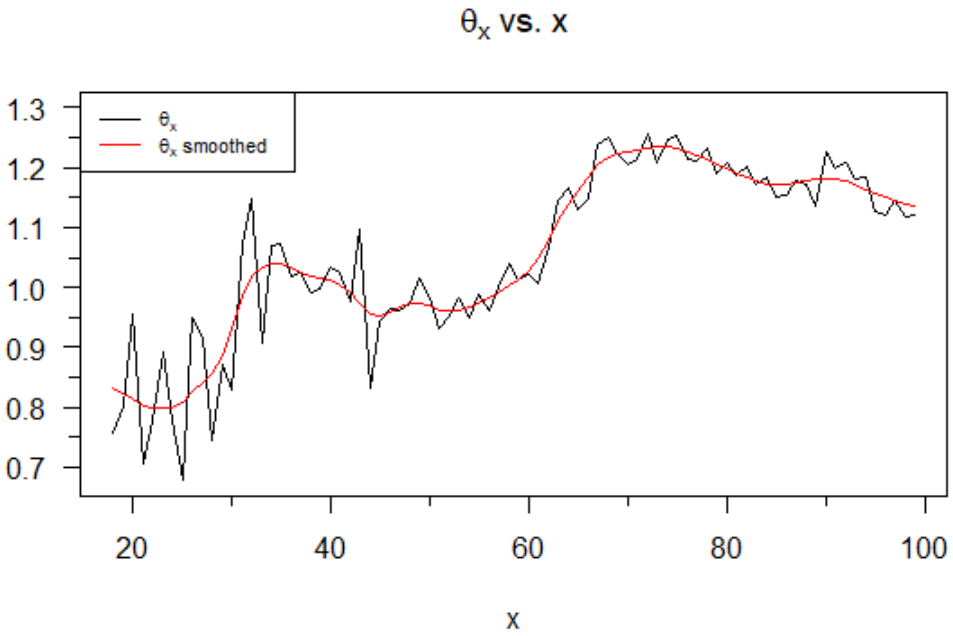

Figure 5.2.3: The process θ_x smoothed for the Belgian population.

We clearly see that θ_x can be divided into 3 groups. One for $20 \rightarrow 30$ where we have $\theta_x < 1$ which means that we have a decrease in mortality compared to the theoretical value. This effect is mostly a consequence due to the lockdown. For the age group $31 \rightarrow 60$, the process θ_x is very close to 1 and for the age group $61 \rightarrow 99$, the process θ_x is higher than 1.

If we look at the process θ_x smoothed decomposed by gender (see Figure 10.3.1 in Appendix C), we see that the excess of mortality is greater for men except for $x > 70$. However for both gender, the process θ_x is less smooth than in Figure 5.2.3.

We can check if the mortality rates obtained with the process θ_x smoothed are close enough to the mortality rates observed for the year 2020. Indeed, for $t = 2020$, we have :

$$\mu_{x,2020}(\text{deformed}) = \mu_{x,2020}(\text{theoretical}) \times \theta_x \tag{5.2.7}$$

and the difference between the two are also shown in Appendix C (Figure 10.3.2).

In conclusion, the scheme of projection for this model is the following :

1. Calibrating a Lee-Carter model on the time period $1980 \rightarrow 2019$.
2. Projecting the parameter κ_t using a random walk with drift.
3. Simulating the binomial variable N_t.
4. Using equation (5.1.5) to obtain the projected mortality rates.

The main benefit of this projection method is that it does not have to deal with the consequence of a jump in the mortality factor κ_t as the calibration time period is limited to 2019. Another interesting feature is that the model can simulate future pandemics based on Covid-19. However, this is also a drawback as we are limited to simulating pandemics with the same characteristics (i.e. the same distribution of excess of mortality over the age) and intensity as Covid-19. This issue will be addressed in the next two chapters.

5.3 Life expectancy and life annuity.

By applying the model described in the previous section, we can calculate the life expectancy and single premium for a life annuity as defined in section 4.2. In Table 5.3.1 and 5.3.2, we display the life expectancies and single premiums obtained for different ages and years with a probability of occurrence of pandemics fixed at 2%. In Appendix C, we show the same result but this time for a probability of occurrence of pandemics fixed at 10%.

We see that for the year 2020, we have almost the same results as those obtained with the observed mortality rates (see Table 4.2.1 and 4.2.2). For the life expectancy in 2050, we see that there is a decrease of about 0.02 years for a person aged 20. This decrease is much smaller than the one obtained by taking the year 2020 in the calibration period. The same observation can be made for single premiums.

Calibration time period: 1980 → 2019

Age	2020	2030	2040	2050
20	**60.71** [60.35 ; 61.06]	**63.46** [62.24 ; 64.56]	**64.98** [63.50 ; 66.35]	**66.35** [64.62 ; 67.88]
40	**41.23** [40.89 ; 41.56]	**43.94** [42.79 ; 44.99]	**45.39** [43.97 ; 46.69]	**46.69** [45.03 ; 48.16]
60	**22.89** [22.59 ; 23.19]	**25.50** [24.44 ; 26.42]	**26.76** [25.46 ; 27.90]	**27.90** [26.42 ; 29.18]
80	**8.16** [8.01 ; 8.30]	**9.61** [9.04 ; 10.11]	**10.29** [9.56 ; 10.92]	**10.92** [10.11 ; 11.65]

Table 5.3.1: Life expectancies calculated with the model for $p = 2\%$.

Calibration time period: 1980 → 2019

Year	Single premium
2020	**15.35** [15.15 ; 15.54]
2030	**17.05** [16.37 ; 17.63]
2040	**17.84** [17.01 ; 18.55]
2050	**18.54** [17.63 ; 19.33]

Table 5.3.2: Single premiums calculated with the model for $p = 2\%$.

Chapter 6

Projection with permanent jump effects.

6.1 Theoretical aspect.

The aim here is to propose another way to take into account the jumps in mortality by working directly on the mortality factor κ_t. This means that if there is a pandemic in year t', the mortality rates in t' become :

$$\mu_{x,t'} = \exp\left(\alpha_x + \beta_x \left(\kappa_{t'} + y\right)\right) \tag{6.1.1}$$

where y is a random variable which expresses the excess of mortality caused by the pandemic. We see in equation (6.1.1) that y is distributed across the age by the parameter β_x. This approach differs from the one in Chapter 5 as we do not explicitly choose how we distribute the excess of mortality across the age and how severe the jumps will be.

In the following we note Y_t, the random variable which gives the value of the jump occurring in year t. This random variable is refereed to as jump severity. Contrary to Chen and Cox (2009) [3] where they only study the case where Y is normally distributed, we also cover the case where we consider an exponential distribution for Y.
There are two main benefits to considering an exponential variable for the jump severity :

- The first one is that an exponential variable is always positive. This can be convenient because pandemics cause positive jumps in the mortality factor.

- The second one is to observe that we only need to estimate one parameter for an exponential distribution whereas we need two parameters for a normal distribution.

In both cases, we assume that Y is independent of the jump frequency variable N where N follows a binomial distribution of parameter p defined in equation (5.1.6).

As suggested by Cox, Lin, and Wang (2006) [4] , a model with permanent jump and with $Y \sim \mathcal{N}(m, s^2)$ describing the evolution of the mortality factor k_t can be written as :

$$\kappa_{t+1} = \kappa_t + \mu - p\,m + \sigma Z_{t+1} + Y_{t+1}N_{t+1} \tag{6.1.2}$$

where μ and σ are constants, and $Z_{t+1} \sim \mathcal{N}(0,1)$ is independent from Y_{t+1} and N_{t+1}.
If we choose $Y \sim \mathcal{E}xp\,(\lambda)$, equation (6.1.2) becomes :

$$\kappa_{t+1} = \kappa_t + \mu - p\,\frac{1}{\lambda} + \sigma Z_{t+1} + Y_{t+1}N_{t+1}. \tag{6.1.3}$$

Equation (6.1.2) and (6.1.3) are said to be permanent jump models because if a jump occurs in $t+1$ (i.e. $N_{t+1} = 1$) the value of Y_{t+1} is then included in κ_{t+1} and this effect will persist for future t.

The calibration of these two equations is done by maximising the log-likelihood function and this function will depend on the distribution chosen for the jump severity variable.

6.1.1 Normally distributed jump variable $Y \sim \mathcal{N}(m, s^2)$

If we assume that the jump severity variable is normally distributed with mean m and variance s^2, then the following proposition holds.

Proposition 6.1.1. *Let us consider the following time series :*

$$z_t = \mu - p\,m + \sigma Z_{t+1} + Y_{t+1}N_{t+1}.$$

The log-likelihood function of this model is then given by :

$$\ln f(z_1, \ldots, z_{K-1}) = \sum_{i=1}^{K-1} \ln \left[\frac{1}{\sqrt{2\pi}S_n} \exp\left(-\frac{(z_i - M_n)^2}{2S_n^2} \right)(1-p) + \frac{1}{\sqrt{2\pi}S_y} \exp\left(-\frac{(z_i - M_y)^2}{2S_y^2} \right) p \right]$$

with

$$\begin{cases} M_n = \mu - pm \\ S_n^2 = \sigma^2 \end{cases} \quad \textit{and} \quad \begin{cases} M_y = \mu + (1-p)m \\ S_y^2 = \sigma^2 + s^2 \end{cases}$$

Proof: We first recall that the density function of a normally distributed variable with mean μ and variance σ^2 is given by :

$$f(x) = \frac{1}{\sqrt{2\pi}\sigma} \exp\left(-\frac{(x-\mu)^2}{2\sigma^2} \right).$$

The equation (6.1.2) can be rewritten as :

$$z_t = \kappa_{t+1} - \kappa_t = \mu - pm + \sigma Z_{t+1} + Y_{t+1}N_{t+1}.$$

If $N_{t+1} = 0$, the variable $z_t|(N_{t+1} = 0)$ will be normally distributed with mean $M_n = \mu - pm$ and variance $S_n^2 = \sigma^2$.
If $N_{t+1} = 1$, the variable $z_t|(N_{t+1} = 1)$ will be normally distributed with mean $M_y = \mu + (1-p)\,m$ and variance $S_y^2 = \sigma^2 + s^2$.
Therefore, the density function of z_t, denoted by $f(z_t)$, can be written in terms of conditional probabilities i.e.,

$$\begin{aligned} f(z_t) &= f(z_t|N_{t+1} = 0)\Pr(N_{t+1} = 0) + f(z_t|N_{t+1} = 1)\Pr(N_{t+1} = 1) \\ &= \frac{1}{\sqrt{2\pi}S_n}\exp\left(-\frac{(z_t - M_n)^2}{2S_n^2}\right) \times (1-p) + \frac{1}{\sqrt{2\pi}S_y}\exp\left(-\frac{(z_t - M_y)^2}{2S_y^2}\right) \times p. \end{aligned}$$

If we have K observations for κ_t, there will be $K-1$ observations for z_t.
The log-likelihood function is then given by :

$$\ln f(z_1, \ldots, z_{K-1}) = \sum_{i=1}^{K-1} \ln f(z_i)$$

which leads to the result.

□

Regarding the parameter p, two solutions are available to us. We can let the parameter be optimise or we can fix it in advance. If we let the parameter p to be optimise we could have the case where the value of p varies considerably depending on the calibration period. In fact, if we do not take the year 2020 in the calibration time period, the value of p tends to be very low. This can be problematic as the probability that a pandemic occurs is not expected to change dramatically from year to year. Therefore, we decide to fix the probability of occurrence in advance by setting $p = 2\%$ for all calibration periods.

6.1.2 Exponentially distributed jump variable $Y \sim \mathcal{E}xp\,(\lambda)$

Before showing the log-likelihood function associated with an exponential distribution for the jump severity variable, we need to derive the density function of a sum of a normal and exponential variable.

Proposition 6.1.2. *If $X \sim \mathcal{N}(\mu, \sigma^2)$ and $Y \sim \mathcal{E}xp\,(\lambda)$, then the density function of $Z = X + Y$ is given by :*

$$f(z) = \lambda \exp\left(\frac{1}{2}\lambda^2\sigma^2 - \lambda(z-\mu)\right)\Phi\left(\frac{(z-\mu) - \lambda\sigma^2}{\sigma}\right)$$

where $\Phi(.)$ is the cumulative density function of a standard normal variable.

Proof: We note respectively $f_Y(y)$ and $f_X(x)$ the density function of the exponential and normal variable. Let us note $f_Z(z)$ the convolution of densities of Y and X :

$$f_Z(z) = \int_{-\infty}^{+\infty} f_Y(y) f_X(z-y) dy.$$

However, we recall that :

$$f_Y(y) = \begin{cases} \lambda\, e^{-\lambda y} & \text{if } y \geq 0 \\ 0 & \text{if } y < 0 \end{cases}$$

$$f_X(z-y) = \frac{1}{\sqrt{2\pi}\sigma} \exp\left(- \frac{\big((z-y)-\mu\big)^2}{2\sigma^2} \right)$$

Therefore we get :

$$\begin{aligned} f_Z(z) &= \lambda \int_0^{+\infty} e^{-\lambda y} \frac{1}{\sqrt{2\pi}\sigma} \exp\left(- \frac{\big((z-y)-\mu\big)^2}{2\sigma^2} \right) dy \\ &= \frac{\lambda}{\sqrt{2\pi}\sigma} \int_0^{+\infty} \exp\left(- \frac{\big((z-y)-\mu\big)^2 + 2\lambda\sigma^2 y}{2\sigma^2} \right) dy. \end{aligned}$$

Given that :

$$\big((z-y)-\mu\big)^2 + 2\lambda\sigma^2 y = \big((z-y)-\mu-\lambda\sigma^2\big)^2 - \big(\lambda\sigma^2\big)^2 + 2\lambda\sigma^2 z - 2\lambda\sigma^2\mu.$$

We can rewrite the expression above as follows :

$$\begin{aligned} f_Z(z) = \frac{\lambda}{\sqrt{2\pi}\sigma} \exp\left(- \frac{-\big(\lambda\sigma^2\big)^2 + 2\lambda\sigma^2 z - 2\lambda\sigma^2\mu}{2\sigma^2} \right) \\ \times \int_0^{+\infty} \exp\left(- \frac{\big((z-y)-\mu-\lambda\sigma^2\big)^2}{2\sigma^2} \right) dy. \end{aligned} \tag{6.1.4}$$

By performing the following substitution, we obtain the relationships hereunder :

$$\begin{cases} v &= \big((z-y)-\mu-\lambda\sigma^2\big) \\ dv &= -dy \end{cases}$$

$$\begin{cases} y &= 0 \quad \longrightarrow \quad v = z-\mu-\lambda\sigma^2 \\ y &= +\infty \quad \longrightarrow \quad v = -\infty \end{cases}$$

As a consequence, the integral in equation (6.1.4) becomes :

$$\begin{aligned}\frac{1}{\sqrt{2\pi}\sigma}\int_0^{+\infty}\exp\left(-\frac{\big((z-y)-\mu-\lambda\sigma^2\big)^2}{2\sigma^2}\right)dy &= \frac{1}{\sqrt{2\pi}\sigma}\int_{z-\mu-\lambda\sigma^2}^{-\infty}\exp\left(-\frac{v^2}{2\sigma^2}\right)(-dv)\\ &= \frac{1}{\sqrt{2\pi}\sigma}\int_{-\infty}^{z-\mu-\lambda\sigma^2}\exp\left(-\frac{v^2}{2\sigma^2}\right)dv\\ &= \Phi\left(\frac{(z-\mu)-\lambda\sigma^2}{\sigma}\right). \qquad (6.1.5)\end{aligned}$$

Combining (6.1.4) and (6.1.5) leads to the result.

□

Thanks to proposition 6.1.2, the log-likelihood function of the model with permanent jump and exponentially distributed jump variable is given above.

Proposition 6.1.3. *Let us consider the following time series :*

$$z_t = \mu - p\,\frac{1}{\lambda} + \sigma Z_{t+1} + Y_{t+1}N_{t+1}.$$

The log-likelihood function of this model is then given by :

$$\begin{aligned}\ln f(z_1,\ldots,z_{K-1}) = \sum_{i=1}^{K-1}\ln\Bigg[&\frac{1}{\sqrt{2\pi}S}\exp\left(-\frac{(z_i-M)^2}{2S^2}\right)(1-p)\\ &+\lambda\exp\left(\frac{1}{2}\lambda^2S^2-\lambda(z_i-M)\right)\Phi\left(\frac{(z_i-M)-\lambda S^2}{S}\right)p\Bigg]\end{aligned}$$

with

$$\begin{cases} M = \mu - p\,\frac{1}{\lambda} \\ S^2 = \sigma^2 \end{cases}$$

Proof: The equation (6.1.3) can be rewritten as :

$$z_t = \kappa_{t+1} - \kappa_t = \mu - p\,\frac{1}{\lambda} + \sigma Z_{t+1} + Y_{t+1}N_{t+1}.$$

If $N_{t+1} = 0$, the variable $z_t|(N_{t+1}=0)$ will be normally distributed with mean $M = \mu - p/\lambda$ and variance $S^2 = \sigma^2$.
If $N_{t+1} = 1$, the variable $z_t|(N_{t+1}=1)$ will be the sum of a normal and exponential variable. Indeed, we have $z_t|(N_{t+1}=1) = X + Y$ with

$$\begin{cases} X \sim \mathcal{N}(M, S^2) \\ Y \sim \mathcal{E}xp\,(\lambda) \end{cases}$$

The proposition 6.1.2 allows to find the density function associated to $z_t|(N_{t+1}=1)$. The density of z_t is then :

$$f(z_t) = f(z_t|N_{t+1}=0)\Pr(N_{t+1}=0) + f(z_t|N_{t+1}=1)\Pr(N_{t+1}=1).$$

Again, if we have K observations for κ_t, there will be $K-1$ observations for z_t.
The log-likelihood function is then given by :

$$\ln f(z_1,\dots,z_{K-1}) = \sum_{i=1}^{K-1} \ln \left[\frac{1}{\sqrt{2\pi}S} \exp\left(-\frac{(z_i-M)^2}{2S^2} \right)(1-p) + \lambda \exp\left(\frac{1}{2}\lambda^2 S^2 - \lambda(z_i - M) \right) \Phi\left(\frac{(z_i-M)-\lambda S^2}{S} \right) p \right]$$

□

As for the normal distribution, we choose to fix the parameter p at 2%.

6.2 Result of the calibration.

Thanks to the propositions 6.1.1 and 6.1.3, we can calibrate the model with permanent jump effects for a normal and exponential distribution. The result of the calibration as well as the AIC and the BIC for the two simulations can be found in Table 6.2.1 and 6.2.2. The result of the calibration with the parameter p free is placed in Appendix D. In the same appendix, we also place the life expectancies and single premiums calculated using mortality rates given by the projection with the permanents jump effects for both distributions and with $p = 2\%$.

In Table 6.2.1, we can see that the impact of Covid-19 has mainly affected the parameters μ and m. The same observation can be made in Table 6.2.2 but with the parameter λ instead of m. Concerning the AIC and BIC, we note that the normal distribution gives the lowest values for the 2 times periods. Comparing with the values in Table 4.1.1, we see that we have a larger AIC and BIC for the time period $1980 \to 2019$ but smaller for the time period $1980 \to 2020$. Nevertheless, the fact that the parameter m is negative for the time period that does not contain the year 2020 is not adequate as we expect pandemics to cause positive jumps. This issue is not present for the exponential distribution.

Concerning the life expectancies and singles premiums. A person aged 20 in 2050 will have a life expectancy equal to 64.48 for the normal distribution and 64.64 for the exponential distribution. For the single premium in 2050, we have 17.56 and 17.64 for each distribution. It can be seen that the choice of distribution has little impact on these two values. These values are slightly higher than those obtained with the basic projection method where we obtain 64.33 for the life expectancy and 17.48 for the single premium if we take the same calibration time period.

Time period	μ	σ	p	m	s
1980 - 2019	-2.0603	2.1518	0.02	-4.1664	0.0045
1980 - 2020	-1.7484	2.2239	0.02	17.4562	0.0008

Time period	AIC	BIC
1980 - 2019	181.43	188.08
1980 - 2020	194.85	201.61

Table 6.2.1: Optimal parameters, AIC and BIC for the model with permanent jump effects and $Y \sim \mathcal{N}(m, s^2)$.

Time period	μ	σ	p	λ
1980 - 2019	-2.0741	2.2417	0.02	15.2289
1980 - 2020	-1.8262	2.2434	0.02	0.0707

Time period	AIC	BIC
1980 - 2019	181.64	188.29
1980 - 2020	198.61	205.36

Table 6.2.2: Optimal parameters, AIC and BIC for the model with permanent jump effects and $Y \sim \mathcal{E}xp\,(\lambda)$.

Nevertheless, one of the drawbacks of the permanent jump model is that most of mortality jumps, such as Covid-19 and the Spanish flu, are caused by normally short-term events. These events would have merely transitory effects on mortality rates. As illustrated in both tables, we still have a decrease of the parameter μ (i.e. the mortality rates will decrease slowly than before in the long term) for both distribution. The next chapter develops the idea of a model taking into account this transitory effects on the mortality rates.

Chapter 7

Projection with transitory jump effects.

7.1 Theoretical aspect.

To represent a model with transitory jump effects on the mortality factor, we use the model developed by Chen and Cox (2009) [3]. Let us first define $\hat{\kappa}_t$, the mortality factor when there is no jump event. We model $\hat{\kappa}_t$ as a random walk with drift :

$$\hat{\kappa}_{t+1} = \hat{\kappa}_t + \mu + \sigma Z_{t+1} \tag{7.1.1}$$

where μ and σ are constants, and $Z_{t+1} \sim \mathcal{N}(0,1)$.
If a jump occurs in year $t+1$ (i.e. $N_{t+1} = 1$), the jump severity variable Y_{t+1} changes the mortality factor from $\hat{\kappa}_{t+1}$ to $\hat{\kappa}_{t+1} + Y_{t+1}$.

$$\kappa_{t+1} = \hat{\kappa}_{t+1} + Y_{t+1}. \tag{7.1.2}$$

If there is no jump in year $t+1$ (i.e. $N_{t+1} = 0$), we have instead :

$$\kappa_{t+1} = \hat{\kappa}_{t+1}. \tag{7.1.3}$$

By combining the equations above, the dynamics of κ_t can be expressed as :

$$\begin{cases} \hat{\kappa}_{t+1} = \hat{\kappa}_t + \mu + \sigma Z_{t+1} \\ \kappa_{t+1} = \hat{\kappa}_{t+1} + Y_{t+1} N_{t+1}. \end{cases} \tag{7.1.4}$$

Eventually, we obtain :

$$\kappa_{t+1} = \kappa_t + \mu + \sigma Z_{t+1} + Y_{t+1} N_{t+1} - Y_t N_t. \tag{7.1.5}$$

Again, the calibration of (7.1.5) is done by maximising the log-likelihood function and will depend on the distribution chosen for Y.

7.1.1 Normally distributed jump variable $Y \sim \mathcal{N}(m, s^2)$

If Y follows a normal distribution, we have the proposition below.

Proposition 7.1.1. *Let us consider the following time series :*

$$z_t = \mu + \sigma Z_{t+1} + Y_{t+1}N_{t+1} - Y_t N_t.$$

The log-likelihood function of this model is then given by :

$$\ln f(z_1, \ldots, z_{K-1}) = \sum_{i=1}^{K-1} \ln \Big[f(z_{i+1}|z_i) \Big] + \ln \Big[f(z_1) \Big]$$

with

$$\begin{aligned}
f(z_{i+1}|z_i) = {} & \frac{1}{\sqrt{2\pi}S_{nn}} \exp\left(- \frac{(z_{i+1} - M_{nn})^2}{2S_{nn}^2} \right) \times (1-p)^2 \\
& + \frac{1}{\sqrt{2\pi}S_{ny}} \exp\left(- \frac{(z_{i+1} - M_{ny})^2}{2S_{ny}^2} \right) \times (1-p)p \\
& + \frac{1}{\sqrt{2\pi}S_{nyn}} \exp\left(- \frac{(z_{i+1} - M_{nyn})^2}{2S_{nyn}^2} \right) \times (1-p)^2 p \\
& + \frac{1}{\sqrt{2\pi}S_{yyn}} \exp\left(- \frac{(z_{i+1} - M_{yyn})^2}{2S_{yyn}^2} \right) \times (1-p)p^2 \\
& + \frac{1}{\sqrt{2\pi}S_{nyy}} \exp\left(- \frac{(z_{i+1} - M_{nyy})^2}{2S_{nyy}^2} \right) \times (1-p)p^2 \\
& + \frac{1}{\sqrt{2\pi}S_{yyy}} \exp\left(- \frac{(z_{i+1} - M_{yyy})^2}{2S_{yyy}^2} \right) \times p^3
\end{aligned}$$

$$\begin{aligned}
f(z_1) = {} & \frac{1}{\sqrt{2\pi}\hat{S}_{nn}} \exp\left(- \frac{(z_1 - \hat{M}_{nn})^2}{2\hat{S}_{nn}^2} \right) \times (1-p)^2 \\
& + \frac{1}{\sqrt{2\pi}\hat{S}_{yn}} \exp\left(- \frac{(z_1 - \hat{M}_{yn})^2}{2\hat{S}_{yn}^2} \right) \times (1-p)p \\
& + \frac{1}{\sqrt{2\pi}\hat{S}_{ny}} \exp\left(- \frac{(z_1 - \hat{M}_{ny})^2}{2\hat{S}_{ny}^2} \right) \times (1-p)p \\
& + \frac{1}{\sqrt{2\pi}\hat{S}_{yy}} \exp\left(- \frac{(z_1 - \hat{M}_{yy})^2}{2\hat{S}_{yy}^2} \right) \times p^2
\end{aligned}$$

$$\begin{cases} M_{nn} = \mu \\ S^2_{nn} = \sigma^2 \end{cases} \quad \begin{cases} M_{ny} = \mu + m \\ S^2_{ny} = \sigma^2 + s^2 \end{cases} \quad \begin{cases} M_{nyn} = -z_i + 2\mu \\ S^2_{nyn} = 2\sigma^2 \end{cases}$$

$$\begin{cases} M_{yyn} = -z_i + 2\mu - m \\ S^2_{yyn} = 2\sigma^2 + s^2 \end{cases} \quad \begin{cases} M_{nyy} = -z_i + 2\mu + m \\ S^2_{nyy} = 2\sigma^2 + s^2 \end{cases} \quad \begin{cases} M_{yyy} = -z_i + 2\mu \\ S^2_{yyy} = 2\sigma^2 + 2s^2 \end{cases}$$

$$\begin{cases} \hat{M}_{nn} = \mu \\ S^2_{nn} = \sigma^2 \end{cases} \quad \begin{cases} \hat{M}_{yn} = \mu - m \\ S^2_{yn} = \sigma^2 + s^2 \end{cases} \quad \begin{cases} \hat{M}_{ny} = \mu + m \\ S^2_{ny} = \sigma^2 + s^2 \end{cases}$$

$$\begin{cases} \hat{M}_{yy} = \mu \\ S^2_{yy} = \sigma^2 + 2s^2 \end{cases}$$

Proof: By posing $z_t = \kappa_{t+1} - \kappa_t$, the equation (7.1.5) can be rewritten as :

$$z_t = \mu + \sigma Z_{t+1} + Y_{t+1}N_{t+1} - Y_t N_t \tag{7.1.6}$$

$$z_{t+1} = \mu + \sigma Z_{t+2} + Y_{t+2}N_{t+2} - Y_{t+1}N_{t+1} \tag{7.1.7}$$

We see that if $N_{t+1} = 0$ then z_t is independent on z_{t+1}.
However, if $N_{t+1} = 1$ then z_t is correlated with z_{t+1}. As a consequence of this observation, we have to use the conditional maximum likelihood estimation (CMLE) to calibrate the parameters.
Under the CMLE, the log-likelihood function is given by :

$$\ln f(z_1, \ldots, z_{K-1}) = \ln f(z_{K-1}|z_{K-2}) + \ln f(z_{K-2}|z_{K-3}) + \ldots + \ln f(z_2|z_1) + \ln f(z_1). \tag{7.1.8}$$

Next, we derive the expression of $f(z_{t+1}|z_t)$ and $f(z_1)$ respectively.
If $N_{t+1} = 0$, the equation (7.1.7) becomes :

$$z_{t+1} = \mu + \sigma Z_{t+2} + Y_{t+2}N_{t+2}.$$

The variable $z_{t+1}|(N_{t+1} = 0, N_{t+2} = 0)$ will be normally distributed with mean $M_{nn} = \mu$ and variance $S^2_{nn} = \sigma^2$.
The variable $z_{t+1}|(N_{t+1} = 0, N_{t+2} = 1)$ will be normally distributed with mean $M_{ny} = \mu + m$ and variance $S^2_{ny} = \sigma^2 + s^2$.
If $N_{t+1} = 1$, by adding Equation (7.1.6) and (7.1.7), we can find the following expression :

$$z_{t+1} = -z_t + 2\mu + \sigma(Z_{t+1} + Z_{t+2}) + Y_{t+2}N_{t+2} - Y_t N_t.$$

The variable $z_{t+1}|(z_t, N_t = 0, N_{t+1} = 1, N_{t+2} = 0)$ will be normally distributed with mean $M_{nyn} = -z_t + 2\mu$ and variance $S^2_{nyn} = 2\sigma^2$.
The variable $z_{t+1}|(z_t, N_t = 1, N_{t+1} = 1, N_{t+2} = 0)$ will be normally distributed with mean $M_{yyn} = -z_t + 2\mu - m$ and variance $S^2_{yyn} = 2\sigma^2 + s^2$.

The variable $z_{t+1}|(z_t, N_t = 0, N_{t+1} = 1, N_{t+2} = 1)$ will be normally distributed with mean $M_{nyy} = -z_t + 2\mu + m$ and variance $S^2_{nyy} = 2\sigma^2 + s^2$.
The variable $z_{t+1}|(z_t, N_t = 0, N_{t+1} = 1, N_{t+2} = 1)$ will be normally distributed with mean $M_{nyy} = -z_t + 2\mu + m$ and variance $S^2_{nyy} = 2\sigma^2 + s^2$.
The variable $z_{t+1}|(z_t, N_t = 1, N_{t+1} = 1, N_{t+2} = 1)$ will be normally distributed with mean $M_{yyy} = -z_t + 2\mu$ and variance $S^2_{yyy} = 2\sigma^2 + 2s^2$.
The conditional density function of $z_{t+1}|z_t$ denoted by $f(z_{t+1}|z_t)$ can then be written as :

$$\begin{aligned}
f(z_{t+1}|z_t) &= f(z_{t+1}|N_{t+1} = 0, N_{t+2} = 0)\Pr(N_{t+1} = 0, N_{t+2} = 0) \\
&\quad + f(z_{t+1}|N_{t+1} = 0, N_{t+2} = 1)\Pr(N_{t+1} = 0, N_{t+2} = 1) \\
&\quad + f(z_{t+1}|z_t, N_t = 0, N_{t+1} = 1, N_{t+2} = 0)\Pr(N_t = 0, N_{t+1} = 1, N_{t+2} = 0) \\
&\quad + f(z_{t+1}|z_t, N_t = 1, N_{t+1} = 1, N_{t+2} = 0)\Pr(N_t = 1, N_{t+1} = 1, N_{t+2} = 0) \\
&\quad + f(z_{t+1}|z_t, N_t = 0, N_{t+1} = 1, N_{t+2} = 1)\Pr(N_t = 0, N_{t+1} = 1, N_{t+2} = 1) \\
&\quad + f(z_{t+1}|z_t, N_t = 1, N_{t+1} = 1, N_{t+2} = 1)\Pr(N_t = 1, N_{t+1} = 1, N_{t+2} = 1) \\
&= \frac{1}{\sqrt{2\pi}S_{nn}} \exp\left(- \frac{(z_{t+1} - M_{nn})^2}{2S^2_{nn}} \right) \times (1-p)^2 \\
&\quad + \frac{1}{\sqrt{2\pi}S_{ny}} \exp\left(- \frac{(z_{t+1} - M_{ny})^2}{2S^2_{ny}} \right) \times (1-p)p \\
&\quad + \frac{1}{\sqrt{2\pi}S_{nyn}} \exp\left(- \frac{(z_{t+1} - M_{nyn})^2}{2S^2_{nyn}} \right) \times (1-p)^2 p \\
&\quad + \frac{1}{\sqrt{2\pi}S_{yyn}} \exp\left(- \frac{(z_{t+1} - M_{yyn})^2}{2S^2_{yyn}} \right) \times (1-p)p^2 \\
&\quad + \frac{1}{\sqrt{2\pi}S_{nyy}} \exp\left(- \frac{(z_{t+1} - M_{nyy})^2}{2S^2_{nyy}} \right) \times (1-p)p^2 \\
&\quad + \frac{1}{\sqrt{2\pi}S_{yyy}} \exp\left(- \frac{(z_{t+1} - M_{yyy})^2}{2S^2_{yyy}} \right) \times p^3
\end{aligned}$$

For z_1, we observe that :

$$z_1 = \mu + \sigma Z_2 + Y_2 N_2 - Y_1 N_1.$$

The variable $z_1|(N_1 = 0, N_2 = 0)$ will be normally distributed with mean $\hat{M}_{nn} = \mu$ and variance $\hat{S}^2_{nn} = \sigma^2$.
The variable $z_1|(N_1 = 1, N_2 = 0)$ will be normally distributed with mean $\hat{M}_{yn} = \mu - m$ and variance $\hat{S}^2_{yn} = \sigma^2 + s^2$.
The variable $z_1|(N_1 = 0, N_2 = 1)$ will be normally distributed with mean $\hat{M}_{ny} = \mu + m$ and variance $\hat{S}^2_{ny} = \sigma^2 + s^2$.
The variable $z_1|(N_1 = 1, N_2 = 1)$ will be normally distributed with mean $\hat{M}_{yy} = \mu$ and

variance $\hat{S}^2_{yy} = \sigma^2 + 2s^2$.
The density function of z_1, which is denoted by $f(z_1)$, can be then written as :

$$\begin{aligned}
f(z_1) &= f(z_1|N_1 = 0, N_2 = 0)\Pr(N_1 = 0, N_2 = 0) \\
&\quad + f(z_1|N_1 = 1, N_2 = 0)\Pr(N_1 = 1, N_2 = 0) \\
&\quad + f(z_1|N_1 = 0, N_2 = 1)\Pr(N_1 = 0, N_2 = 1) \\
&\quad + f(z_1|N_1 = 1, N_2 = 1)\Pr(N_1 = 1, N_2 = 1) \\
&= \frac{1}{\sqrt{2\pi}\hat{S}_{nn}} \exp\left(- \frac{(z_1 - \hat{M}_{nn})^2}{2\hat{S}^2_{nn}} \right) \times (1-p)^2 \\
&\quad + \frac{1}{\sqrt{2\pi}\hat{S}_{yn}} \exp\left(- \frac{(z_1 - \hat{M}_{yn})^2}{2\hat{S}^2_{yn}} \right) \times (1-p)p \\
&\quad + \frac{1}{\sqrt{2\pi}\hat{S}_{ny}} \exp\left(- \frac{(z_1 - \hat{M}_{ny})^2}{2\hat{S}^2_{ny}} \right) \times (1-p)p \\
&\quad + \frac{1}{\sqrt{2\pi}\hat{S}_{yy}} \exp\left(- \frac{(z_1 - \hat{M}_{yy})^2}{2\hat{S}^2_{yy}} \right) \times p^2
\end{aligned}$$

Substituting the formulas of $f(z_{t+1}|z_t)$ and $f(z_1)$ into equation (7.1.8) we obtain the log-likelihood function.

□

As for the projection with permanent jump effects, we fix in advance the parameter p equal to 2%. We will also do the same assumption for $Y \sim \mathcal{E}\mathrm{xp}\,(\lambda)$.

7.1.2 Exponentially distributed jump variable $Y \sim \mathcal{E}xp\,(\lambda)$

As a reminder, if $X \sim \mathcal{N}(\mu, \sigma^2)$ and $Y \sim \mathcal{E}xp\,(\lambda)$ then the proposition 6.1.2 shows the density function of $Z = X + Y$. In the following, we derive other useful densities that we will use in the calculation of the log-likelihood function of the model.

Proposition 7.1.2. *If $X \sim \mathcal{N}(\mu, \sigma^2)$ and $Y \sim \mathcal{E}xp\,(\lambda)$, then the density function of $Z = X - Y$ is given by :*

$$f(z) = \lambda \exp\left(\frac{1}{2}\lambda^2\sigma^2 + \lambda\big(z - \mu\big)\right)\left(1 - \Phi\left(\frac{(z-\mu) + \lambda\sigma^2}{\sigma}\right)\right).$$

where $\Phi(.)$ is the cumulative density function of a standard normal variable.

Proof: The proof is similar to the proposition 6.1.2 except that the convolution of densities of Y and X is given by :

$$f_Z(z) = \int_{-\infty}^{+\infty} f_Y(y) f_X(z+y) dy.$$

Therefore we get :

$$f_Z(z) = \frac{\lambda}{\sqrt{2\pi}\sigma} \int_0^{+\infty} \exp\left(- \frac{\big((z+y)-\mu\big)^2 + 2\lambda\sigma^2 y}{2\sigma^2} \right) dy. \tag{7.1.9}$$

Given that :

$$\big((z+y)-\mu\big)^2 + 2\lambda\sigma^2 y = \big((z+y)-\mu+\lambda\sigma^2\big)^2 - \big(\lambda\sigma^2\big)^2 - 2\lambda\sigma^2 z + 2\lambda\sigma^2\mu.$$

With this result, we can rewrite equation (7.1.9) as follows :

$$\begin{aligned} f_Z(z) = \frac{\lambda}{\sqrt{2\pi}\sigma} \exp\left(- \frac{-\big(\lambda\sigma^2\big)^2 - 2\lambda\sigma^2 z + 2\lambda\sigma^2\mu}{2\sigma^2} \right) \\ \times \int_0^{+\infty} \exp\left(- \frac{\big((z+y)-\mu+\lambda\sigma^2\big)^2}{2\sigma^2} \right) dy \end{aligned} \tag{7.1.10}$$

By performing the following substitution, we obtain the relationships hereunder :

$$\begin{cases} v &= \big((z+y)-\mu+\lambda\sigma^2\big) \\ dv &= dy \end{cases}$$

$$\begin{cases} y &= 0 \quad \longrightarrow \quad v = z-\mu+\lambda\sigma^2 \\ y &= +\infty \quad \longrightarrow \quad v = +\infty \end{cases}$$

As a consequence, the integral in equation (7.1.10) becomes :

$$\begin{aligned} \frac{1}{\sqrt{2\pi}\sigma} \int_0^{+\infty} \exp\left(- \frac{\big((z+y)-\mu+\lambda\sigma^2\big)^2}{2\sigma^2} \right) dy &= \frac{1}{\sqrt{2\pi}\sigma} \int_{z-\mu+\lambda\sigma^2}^{+\infty} \exp\left(- \frac{v^2}{2\sigma^2} \right) dv \\ &= 1 - \Phi\left(\frac{(z-\mu)+\lambda\sigma^2}{\sigma} \right) \end{aligned} \tag{7.1.11}$$

Combining equation (7.1.10) and (7.1.11) leads to the result.

□

Proposition 7.1.3. *If $X \sim \mathcal{E}xp(\lambda)$ and $Y \sim \mathcal{E}xp(\lambda)$, then the density function of $Z = X - Y$ is given by :*

$$f(z) = \frac{\lambda}{2}\left[e^{-\lambda z}\,\mathbf{1}_{\{z\geq 0\}} + e^{\lambda z}\,\mathbf{1}_{\{z<0\}} \right]$$

where $\mathbf{1}_{\{.\}}$ is the indicator function.

Proof: Let us note $f_Z(z)$ the convolution of densities of Y and X :

$$f_Z(z) = \int_{-\infty}^{+\infty} f_Y(y) f_X(z+y) dy. \tag{7.1.12}$$

The density of Y and X are given by :

$$f_Y(y) = \begin{cases} \lambda\, e^{-\lambda y} & \text{if } y \geq 0 \\ 0 & \text{if } y < 0 \end{cases}$$
$$f_X(z+y) = \begin{cases} \lambda\, e^{-\lambda(z+y)} & \text{if } z+y \geq 0 \\ 0 & \text{if } z+y < 0 \end{cases}$$

$z + y \geq 0$ means that $y \geq -z$ and $z + y < 0$ means that $y < -z$.
By replacing in equation (7.1.12), we obtain :

$$\begin{aligned} f_Z(z) &= \int_0^{+\infty} \lambda\, e^{-\lambda y} \lambda\, e^{-\lambda(z+y)}\, \mathbf{1}_{\{z\geq 0\}}\, dy + \int_{-z}^{+\infty} \lambda\, e^{-\lambda y} \lambda\, e^{-\lambda(z+y)}\, \mathbf{1}_{\{z<0\}}\, dy \\ &= \lambda^2\, e^{-\lambda z} \int_0^{+\infty} e^{-2\lambda y}\, dy\, \mathbf{1}_{\{z\geq 0\}} + \lambda^2\, e^{-\lambda z} \int_{-z}^{+\infty} e^{-2\lambda y}\, dy\, \mathbf{1}_{\{z<0\}} \\ &= \frac{\lambda\, e^{-\lambda z}}{2} \left[\mathbf{1}_{\{z\geq 0\}} + e^{2\lambda z}\, \mathbf{1}_{\{z<0\}} \right] \end{aligned}$$

Eventually, we obtain the density distribution :

$$f_Z(z) = \frac{\lambda}{2} \left[e^{-\lambda z}\, \mathbf{1}_{\{z\geq 0\}} + e^{\lambda z}\, \mathbf{1}_{\{z<0\}} \right].$$

□

Proposition 7.1.4. *If $X \sim \mathcal{N}(\mu, \sigma^2)$ and $Y \sim \mathcal{E}xp(\lambda)$, then the density function of $Z = X + Y - Y$ is given by :*

$$\begin{aligned} f(z) = &\frac{\lambda}{2} \exp\left(\frac{1}{2}\lambda^2\sigma^2 - \lambda(z-\mu) \right) \Phi\left(\frac{(z-\mu) - \lambda\sigma^2}{\sigma} \right) \\ &+ \frac{\lambda}{2} \exp\left(\frac{1}{2}\lambda^2\sigma^2 + \lambda(z-\mu) \right) \left(1 - \Phi\left(\frac{(z-\mu) - \lambda\sigma^2}{\sigma} \right) \right) \end{aligned}$$

where $\Phi(.)$ is the cumulative density function of a standard normal variable.

Proof: Recall that the density function of $\hat{Y} = Y - Y$ is known from the proposition 7.1.3.

$$f_{\hat{Y}}(\hat{y}) = \begin{cases} \frac{\lambda}{2}\, e^{-\lambda y} & \text{if } \hat{y} \geq 0 \\ \frac{\lambda}{2}\, e^{\lambda y} & \text{if } \hat{y} < 0 \end{cases}$$

Then Z can be written as $Z = X + Y - Y = X + \hat{Y}$.
If we note $f_Z(z)$ the convolution of densities of X and $\hat{Y}$, we have :

$$f_Z(z) = \int_{-\infty}^{+\infty} f_{\hat{Y}}(\hat{y}) f_X(z - \hat{y}) d\hat{y} \tag{7.1.13}$$

and $f_X(z - \hat{y})$ is given by :

$$f_X(z - \hat{y}) = \frac{1}{\sqrt{2\pi}\sigma} \exp\left(- \frac{\big((z - \hat{y}) - \mu\big)^2}{2\sigma^2} \right).$$

Newt, equation (7.1.13) becomes :

$$\begin{aligned} f_Z(z) &= \frac{\lambda}{2\sqrt{2\pi}\sigma} \int_0^{+\infty} e^{-\lambda\hat{y}} \exp\left(- \frac{\big((z - \hat{y}) - \mu\big)^2}{2\sigma^2} \right) d\hat{y} \\ &\quad + \frac{\lambda}{2\sqrt{2\pi}\sigma} \int_{-\infty}^{0} e^{\lambda\hat{y}} \exp\left(- \frac{\big((z - \hat{y}) - \mu\big)^2}{2\sigma^2} \right) d\hat{y} \\ &= A + B \end{aligned}$$

For A we have :

$$A = \frac{\lambda}{2\sqrt{2\pi}\sigma} \int_0^{+\infty} \exp\left(- \frac{\big((z - \hat{y}) - \mu\big)^2 + 2\lambda\sigma^2\hat{y}}{2\sigma^2} \right) d\hat{y}$$

which is the same integral obtained in the proof of the proposition 6.1.2.
Therefore, we obtain :

$$A = \frac{\lambda}{2} \exp\left(\frac{1}{2}\lambda^2\sigma^2 - \lambda(z - \mu) \right) \Phi\left(\frac{(z - \hat{y}) - \lambda\sigma^2}{\sigma} \right). \tag{7.1.14}$$

For B we have :

$$B = \frac{\lambda}{2\sqrt{2\pi}\sigma} \int_{-\infty}^{0} \exp\left(- \frac{\big((z - \hat{y}) - \mu\big)^2 - 2\lambda\sigma^2\hat{y}}{2\sigma^2} \right) d\hat{y}.$$

Given that :

$$\big((z - \hat{y}) - \mu\big)^2 - 2\lambda\sigma^2\hat{y} = \big((z - \hat{y}) - \mu + \lambda\sigma^2\big)^2 - \big(\lambda\sigma^2\big)^2 - 2\lambda\sigma^2 z + 2\lambda\sigma^2\mu.$$

We can rewrite B as follows :

$$B = \frac{\lambda}{2\sigma\sqrt{2\pi}} \exp\left(- \frac{-\left(\lambda\sigma^2\right)^2 - 2\lambda\sigma^2(z-\mu)}{2\sigma^2} \right) \times \int_{-\infty}^{0} \exp\left(- \frac{\left((z-\hat{y}) - \mu + \lambda\sigma^2\right)^2}{2\sigma^2} \right) d\hat{y} \tag{7.1.15}$$

By performing the following substitution, we obtain the relationships hereunder :

$$\begin{cases} v &= \left((z-\hat{y}) - \mu + \lambda\sigma^2\right) \\ dv &= -d\hat{y} \end{cases}$$

$$\begin{cases} y &= 0 \quad \longrightarrow \quad v = z - \mu + \lambda\sigma^2 \\ y &= -\infty \quad \longrightarrow \quad v = +\infty \end{cases}$$

As a consequence, the integral in equation (7.1.15) becomes :

$$\begin{aligned} \frac{1}{\sqrt{2\pi}\sigma} \int_{-\infty}^{0} \exp\left(- \frac{\left((z-\hat{y}) - \mu + \lambda\sigma^2\right)^2}{2\sigma^2} \right) d\hat{y} &= \frac{1}{\sqrt{2\pi}\sigma} \int_{+\infty}^{z-\mu+\lambda\sigma^2} \exp\left(- \frac{v^2}{2\sigma^2} \right) (-dv) \\ &= \frac{1}{\sqrt{2\pi}\sigma} \int_{z-\mu+\lambda\sigma^2}^{+\infty} \exp\left(- \frac{v^2}{2\sigma^2} \right) dv \\ &= \left(1 - \Phi\left(\frac{z-\mu+\lambda\sigma^2}{\sigma} \right) \right) \end{aligned}$$

Eventually, we obtain for B :

$$B = \frac{\lambda}{2} \exp\left(\frac{1}{2}\lambda^2\sigma^2 + \lambda(z-\mu) \right) \left(1 - \Phi\left(\frac{z-\mu+\lambda\sigma^2}{\sigma} \right) \right). \tag{7.1.16}$$

By combining equation (7.1.14) and (7.1.16), we find the density function of Z.

□

The propositions 6.1.2, 7.1.2, 7.1.3 and 7.1.4 will allows us to derive the log-likelihood function of the model with the projection with transitory jump effects and $Y \sim \mathcal{E}\mathrm{xp}\,(\lambda)$:

Proposition 7.1.5. *Let us consider the following time series :*

$$z_t = \mu + \sigma Z_{t+1} + Y_{t+1}N_{t+1} - Y_t N_t.$$

The log-likelihood function of this model is then given by :

$$\ln f(z_1, \ldots, z_{K-1}) = \sum_{i=1}^{K-1} \ln\left[f(z_{i+1}|z_i) \right] + \ln\left[f(z_1) \right]$$

with

$$
\begin{aligned}
f(z_{i+1}|z_i) = {} & \frac{1}{\sqrt{2\pi}S}\exp\left(-\frac{(z_{t+1}-M)^2}{2S^2}\right)\times(1-p)^2 \\
& + \lambda\exp\left(\frac{1}{2}\lambda^2S^2-\lambda(z-M)\right)\Phi\left(\frac{(z-M)-\lambda S^2}{S}\right)\times(1-p)p \\
& + \frac{1}{\sqrt{2\pi}\hat{S}}\exp\left(-\frac{(z_{t+1}-\hat{M})^2}{2\hat{S}^2}\right)\times(1-p)^2p \\
& + \lambda\exp\left(\frac{1}{2}\lambda^2\hat{S}^2+\lambda\big(z-\hat{M}\big)\right)\left(1-\Phi\left(\frac{(z-\hat{M})+\lambda S^2}{S}\right)\right)\times(1-p)p^2 \\
& + \lambda\exp\left(\frac{1}{2}\lambda^2\hat{S}^2-\lambda(z-\hat{M})\right)\Phi\left(\frac{(z-\hat{M})-\lambda\hat{S}^2}{\hat{S}}\right)\times(1-p)p^2 \\
& + \left[\frac{\lambda}{2}\exp\left(\frac{1}{2}\lambda^2\hat{S}^2-\lambda(z-\hat{M})\right)\Phi\left(\frac{(z-\hat{M})-\lambda\hat{S}^2}{\hat{S}}\right)\right. \\
& \left. + \frac{\lambda}{2}\exp\left(\frac{1}{2}\lambda^2\hat{S}^2+\lambda(z-\hat{M})\right)\left(1-\Phi\left(\frac{(z-\hat{M})-\lambda\hat{S}^2}{\hat{S}}\right)\right)\right]\times p^3
\end{aligned}
$$

$$
\begin{aligned}
f(z_1) = {} & \frac{1}{\sqrt{2\pi}S}\exp\left(-\frac{(z_1-M)^2}{2S^2}\right)\times(1-p)^2 \\
& + \lambda\exp\left(\frac{1}{2}\lambda^2S^2+\lambda\big(z-M\big)\right)\left(1-\Phi\left(\frac{(z-M)+\lambda S^2}{S}\right)\right)\times(1-p)p \\
& + \lambda\exp\left(\frac{1}{2}\lambda^2S^2-\lambda(z-M)\right)\Phi\left(\frac{(z-M)-\lambda S^2}{S}\right)\times(1-p)p \\
& + \left[\frac{\lambda}{2}\exp\left(\frac{1}{2}\lambda^2S^2-\lambda(z-M)\right)\Phi\left(\frac{(z-M)-\lambda S^2}{S}\right)\right. \\
& \left. + \frac{\lambda}{2}\exp\left(\frac{1}{2}\lambda^2S^2+\lambda(z-M)\right)\left(1-\Phi\left(\frac{(z-M)-\lambda S^2}{S}\right)\right)\right]\times p^2
\end{aligned}
$$

$$
\left\{\begin{array}{l} M=\mu \\ S^2=\sigma^2 \end{array}\right. \qquad \textit{and} \qquad \left\{\begin{array}{l} \hat{M}=-z_t+2\mu \\ \hat{S}^2=2\sigma^2 \end{array}\right.
$$

Proof: By posing $z_t = \kappa_{t+1} - \kappa_t$, the equation (7.1.5) can be rewritten as :

$$z_t = \mu + \sigma Z_{t+1} + Y_{t+1}N_{t+1} - Y_tN_t \tag{7.1.17}$$

$$z_{t+1} = \mu + \sigma Z_{t+2} + Y_{t+2}N_{t+2} - Y_{t+1}N_{t+1} \tag{7.1.18}$$

We see that if $N_{t+1} = 0$ then z_t is independent on z_{t+1}.
However, if $N_{t+1} = 1$ then z_t is correlated with z_{t+1}. As a consequence of this observation, we need to use the conditional maximum likelihood estimation (CMLE) to calibrate the parameters.
Under the CMLE, the log-likelihood function is given by :

$$\ln f(z_1, \ldots, z_{K-1}) = \ln f(z_{K-1}|z_{K-2}) + \ln f(z_{K-2}|z_{K-3}) + \ldots + \ln f(z_2|z_1) + \ln f(z_1). \tag{7.1.19}$$

Next, we derive the expression of $f(z_{t+1}|z_t)$ and $f(z_1)$ respectively.
If $N_{t+1} = 0$, then we have :

$$z_{t+1} = \mu + \sigma Z_{t+2} + Y_{t+2} N_{t+2}.$$

The variable $z_{t+1}|(N_{t+1} = 0, N_{t+2} = 0)$ will be normally distributed with mean $M = \mu$ and variance $S^2 = \sigma^2$.
The variable $z_{t+1}|(N_{t+1} = 0, N_{t+2} = 1)$ will be the sum of a normal and exponential variable. Indeed, we have $z_{t+1}|(N_{t+1} = 0, N_{t+2} = 1) = X + Y$ with :

$$\begin{cases} X \sim \mathcal{N}(M, S^2) \\ Y \sim \mathcal{E}xp\,(\lambda) \end{cases}$$

If $N_{t+1} = 1$, by adding the equations (7.1.17) and (7.1.18), we can find the following expression :

$$z_{t+1} = -z_t + 2\mu + \sigma(Z_{t+1} + Z_{t+2}) + Y_{t+2} N_{t+2} - Y_t N_t.$$

The variable $z_{t+1}|(z_t, N_t = 0, N_{t+1} = 1, N_{t+2} = 0)$ will be normally distributed with mean $\hat{M} = -z_t + 2\mu$ and variance $\hat{S}^2 = 2\sigma^2$.
The variable $z_{t+1}|(z_t, N_t = 1, N_{t+1} = 1, N_{t+2} = 0)$ will be the difference of a normal and an exponential variable. Indeed, we have $z_{t+1}|(z_t, N_t = 1, N_{t+1} = 1, N_{t+2} = 0) = \hat{X} - \hat{Y}$ with :

$$\begin{cases} \hat{X} \sim \mathcal{N}(\hat{M}, \hat{S}^2) \\ \hat{Y} \sim \mathcal{E}xp\,(\lambda) \end{cases}$$

The variable $z_{t+1}|(z_t, N_t = 0, N_{t+1} = 1, N_{t+2} = 1)$ will be the sum of a normal and an exponential variable. Indeed, we have $z_{t+1}|(z_t, N_t = 0, N_{t+1} = 1, N_{t+2} = 1) = \hat{X} + \hat{Y}$.
The variable $z_{t+1}|(z_t, N_t = 1, N_{t+1} = 1, N_{t+2} = 1)$ will be a combination of a normal and two exponential variables. Indeed, we have $z_{t+1}|(z_t, N_t = 1, N_{t+1} = 1, N_{t+2} = 1) = \hat{X} + \hat{Y} - \hat{Y}$.

The conditional density function of $z_{t+1}|z_t$ denoted by $f(z_{t+1}|z_t)$ can then be written as :

$$
\begin{aligned}
f(z_{t+1}|z_t) &= f(z_{t+1}|N_{t+1}=0,N_{t+2}=0)\Pr(N_{t+1}=0,N_{t+2}=0)\\
&\quad + f(z_{t+1}|N_{t+1}=0,N_{t+2}=1)\Pr(N_{t+1}=0,N_{t+2}=1)\\
&\quad + f(z_{t+1}|z_t,N_t=0,N_{t+1}=1,N_{t+2}=0)\Pr(N_t=0,N_{t+1}=1,N_{t+2}=0)\\
&\quad + f(z_{t+1}|z_t,N_t=1,N_{t+1}=1,N_{t+2}=0)\Pr(N_t=1,N_{t+1}=1,N_{t+2}=0)\\
&\quad + f(z_{t+1}|z_t,N_t=0,N_{t+1}=1,N_{t+2}=1)\Pr(N_t=0,N_{t+1}=1,N_{t+2}=1)\\
&\quad + f(z_{t+1}|z_t,N_t=1,N_{t+1}=1,N_{t+2}=1)\Pr(N_t=1,N_{t+1}=1,N_{t+2}=1)\\
&= \frac{1}{\sqrt{2\pi}S}\exp\left(-\frac{(z_{t+1}-M)^2}{2S^2}\right)\times(1-p)^2\\
&\quad + \lambda\exp\left(\frac{1}{2}\lambda^2S^2-\lambda(z-M)\right)\Phi\left(\frac{(z-M)-\lambda S^2}{S}\right)\times(1-p)p\\
&\quad + \frac{1}{\sqrt{2\pi}\hat{S}}\exp\left(-\frac{(z_{t+1}-\hat{M})^2}{2\hat{S}^2}\right)\times(1-p)^2p\\
&\quad + \lambda\exp\left(\frac{1}{2}\lambda^2\hat{S}^2+\lambda\big(z-\hat{M}\big)\right)\left(1-\Phi\left(\frac{(z-\hat{M})+\lambda S^2}{S}\right)\right)\times(1-p)p^2\\
&\quad + \lambda\exp\left(\frac{1}{2}\lambda^2\hat{S}^2-\lambda(z-\hat{M})\right)\Phi\left(\frac{(z-\hat{M})-\lambda\hat{S}^2}{\hat{S}}\right)\times(1-p)p^2\\
&\quad + \left[\frac{\lambda}{2}\exp\left(\frac{1}{2}\lambda^2\hat{S}^2-\lambda(z-\hat{M})\right)\Phi\left(\frac{(z-\hat{M})-\lambda\hat{S}^2}{\hat{S}}\right)\right.\\
&\quad \left. + \frac{\lambda}{2}\exp\left(\frac{1}{2}\lambda^2\hat{S}^2+\lambda(z-\hat{M})\right)\left(1-\Phi\left(\frac{(z-\hat{M})-\lambda\hat{S}^2}{\hat{S}}\right)\right)\right]\times p^3
\end{aligned}
$$

For z_1, we observe that :

$$z_1 = \mu + \sigma Z_2 + Y_2N_2 - Y_1N_1.$$

The variable $z_1|(N_1=0,N_2=0)$ will be normally distributed with mean $M=\mu$ and variance $S^2=\sigma^2$.
The variable $z_1|(N_1=1,N_2=0)$ will be the difference of a normal and an exponential variable. Indeed, we have $z_1|(N_1=1,N_2=0)=X-Y$.
The variable $z_1|(N_1=0,N_2=1)$ will be the sum of a normal and an exponential variable. Indeed, we have $z_1|(N_1=0,N_2=1)=X+Y$.
The variable $z_1|(N_1=1,N_2=1)$ will be a combination of a normal and two exponential variables. Indeed, we have $z_1|(N_1=1,N_2=1)=X+Y-Y$.

The density function of z_1, which is denoted by $f(z_1)$, can be then written as :

$$\begin{aligned}
f(z_1) &= f(z_1|N_1=0,N_2=0)\Pr(N_1=0,N_2=0)\\
&\quad + f(z_1|N_1=1,N_2=0)\Pr(N_1=1,N_2=0)\\
&\quad + f(z_1|N_1=0,N_2=1)\Pr(N_1=0,N_2=1)\\
&\quad + f(z_1|N_1=1,N_2=1)\Pr(N_1=1,N_2=1)\\
&= \frac{1}{\sqrt{2\pi}S}\exp\left(-\frac{(z_1-M)^2}{2S^2}\right)\times(1-p)^2\\
&\quad + \lambda\exp\left(\frac{1}{2}\lambda^2S^2+\lambda\big(z-M)\big)\right)\left(1-\Phi\left(\frac{(z-M)+\lambda S^2}{S}\right)\right)\times(1-p)p\\
&\quad + \lambda\exp\left(\frac{1}{2}\lambda^2S^2-\lambda(z-M)\right)\Phi\left(\frac{(z-M)-\lambda S^2}{S}\right)\times(1-p)p\\
&\quad + \left[\frac{\lambda}{2}\exp\left(\frac{1}{2}\lambda^2S^2-\lambda(z-M)\right)\Phi\left(\frac{(z-M)-\lambda S^2}{S}\right)\right.\\
&\quad \left.+\frac{\lambda}{2}\exp\left(\frac{1}{2}\lambda^2S^2+\lambda(z-M)\right)\left(1-\Phi\left(\frac{(z-M)-\lambda S^2}{S}\right)\right)\right]\times p^2
\end{aligned}$$

Substituting the formulas of $f(z_{t+1}|z_t)$ and $f(z_1)$ into (7.1.19) and we obtain the log-likelihood function.

□

7.2 Result of the calibration.

Thanks to the propositions 7.1.1 and 7.1.5, we can calibrate the model with transitory jump effects for a normal and exponential distribution. The result of the calibration as well as the AIC and the BIC for the two simulations can be found in Table 7.2.1 and 7.2.2. The result of the calibration with the parameter p free is placed in Appendix E. In the same appendix, we also place the life expectancies and single premiums calculated using mortality rates given by the projection with transitory jump effects for both distributions.

In Table 7.2.1, we can see that the impact of Covid-19 has mainly affected the parameters and m and no longer the parameter μ as for the model with permanent jump effects. The same observation can be made in Table 7.2.2 but with the parameter λ instead of m. Concerning the AIC and BIC, we note that the exponential distribution gives the lowest values for the time period $1980 \to 2019$ and the normal distribution gives the lowest values for the time period taking the year 2020 into account. Comparing with the values in Table 4.1.1, we see that we have a larger AIC and BIC for the time period $1980 \to 2019$ but smaller for the time period $1980 \to 2020$. However, if we compare these values with

those obtained with the permanent jump effects model, we have slightly higher values for both distributions and both time periods. Nevertheless, as for the permanent model, the parameter m is still negative for the time period $1980 \rightarrow 2019$.

Concerning the life expectancies and singles premiums. A person aged 20 in 2050 will have a life expectancy equal to 65.22 for the normal distribution and 65.29 for the exponential distribution. For the single premium in 2050, we have 17.95 and 17.98 for each distribution. It can be seen that the choice of distribution has little impact on these two values. These values are higher than those obtained with the basic projection method and the model with permanent jump effects. In fact, the values obtained with the transitory jump effects are very close to those obtained with the basic projection method for the calibration time period $1980 \rightarrow 2019$. As a reminder, we obtained 66.37 and 18.56 for this time period. This was expected as the parameter μ was nearly the same for the two calibration time periods.

Time period	μ	σ	p	m	s
1980 - 2019	-1.9778	2.1584	0.02	-4.1403	0.0005
1980 - 2020	-2.0951	2.2285	0.02	17.4491	0.0008

Time period	AIC	BIC
1980 - 2019	184.22	192.54
1980 - 2020	197.70	206.15

Table 7.2.1: Optimal parameters, AIC and BIC for the model with transitory jump effects and $Y \sim \mathcal{N}(m, s^2)$.

Time period	μ	σ	p	λ
1980 - 2019	-2.0808	2.2437	0.02	2.2597
1980 - 2020	-2.1066	2.2484	0.02	0.0707

Time period	AIC	BIC
1980 - 2019	182.40	189.06
1980 - 2020	199.42	206.18

Table 7.2.2: Optimal parameters, AIC and BIC for the model with transitory jump effects and $Y \sim \mathcal{E}\text{xp}\,(\lambda)$.

Chapter 8

Multi-population models.

8.1 Theoretical aspect.

In the previous chapters, we focused our study on the Lee-Carter model. In what follows, we will focus on a multi-population model which is an extension of the classical Lee-Carter model. In a multi-population model, the idea is that closely related populations tend to have the same mortality trends over time. Indeed, jointly fitting a mortality model on two countries sharing the same economic and demographic development would tend to decrease the uncertainty of the parameters. This will avoid the long-term discrepancies in mortality projections that can occur if we fit two separate mortality models, one for each population.

Li & Lee (2005) [8] introduced an approach to jointly calibrate a stochastic mortality model across several populations and to guarantee the long-term non-divergence of the projection. Li & Lee model suggests that the mortality rates of country i can be written as :

$$\ln \mu_{x,t}(i) = \alpha_x(i) + \beta_x(i)\, \kappa_t(i) + B_x\, K_t \tag{8.1.1}$$

where

- $B_x\, K_t$ is the common time trend.
- $\alpha_x(i) + \beta_x(i)\, \kappa_t(i)$ is the population-specific factor that allows populations to deviate from the common main trend.

The calibration is performed by first fitting a Lee-Carter model on the reference population (i.e. the population we choose as reference) to find the parameters K_t and B_x. Then we find the parameters $\alpha_x(i)$, $\beta_x(i)$ and $\kappa_t(i)$ using the SVD[1] algorithm. We also impose a set of constraints to ensure that the model is identifiable :

$$\begin{cases} \sum_x B_x = 1 \\ \sum_t K_t = 0 \end{cases} \qquad \begin{cases} \sum_x \beta_x(i) = 1 \\ \sum_t \kappa_t(i) = 0 \end{cases}$$

The function *model.LiLee(.)* from the R-package **MortalityForecast** uses this methodology to calibrate the Li & Lee model defined in equation (8.1.1). We will use this function to calibrate the model and the R-package **MortalityForecast** can be found here[2].

8.2 Calibration.

Before showing the result of the calibration, we need to define our reference population, i.e. the population that will give us the parameters K_t and B_x. For this dissertation, we have chosen to take as reference population the combination of the Belgian and the Dutch population. The data for the Dutch population are taken from the same database as the Belgian population, i.e. HMD. Unfortunately, the data for the year 2020 for the Dutch population is not yet available at the time of writing this thesis. The reader can find the methodology we use to overcome this problem and how we construct the data for the year 2020 in Appendix F.

Once we have the database for the benchmark population, we can fit the Li & Lee model in order to find the mortality rates for the Belgium population. We take the same time period and age group as for the Lee-Carter model :

- ☐ $1980 \rightarrow 2020$
- ☐ $0 \rightarrow 99$

The parameters found by the calibration are displayed in Figure 8.2.1.
We see that the impact of Covid-19 is less severe in the Lee & Li model than in the Lee-Carter model. Indeed, the excess mortality observed during the year 2020 is divided into two parameters: K_t and $\kappa_t(BE)$ which means that any jump in mortality is spread over these two parameters. Apart for the year 2020, we can see that we have a regular decrease of K_t as for the mortality factor κ_t of the classical Lee-Carter model. The parameter $\kappa_t(BE)$ is more difficult to interpret because it varies a lot over the period but we can see that it oscillates around 0.

[1] Singular value decomposition.
[2] `https://github.com/mpascariu/MortalityForecast`

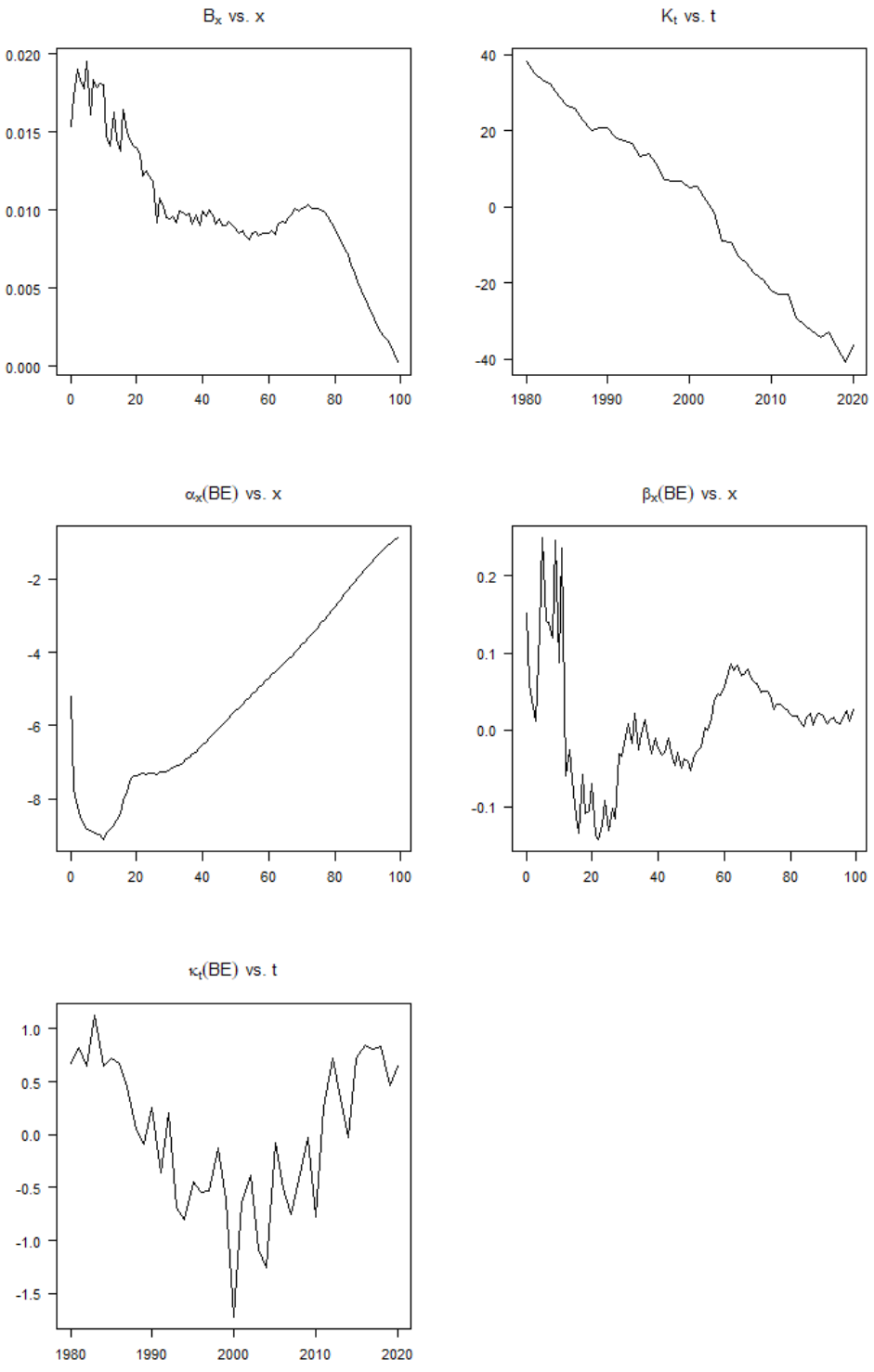

Figure 8.2.1: Calibration of the Li & Lee model for the Belgian population with Dutch and Belgian population as benchmark.

8.3 Projection without jump effects.

Unlike the Lee-Carter model, the Li & Lee model requires the simulation of two time series (K_t and $\kappa_t(i)$). In their paper, Li & Lee recommend using a random walk with drift for K_t and a random walk without drift (i.e. RW) or a first-order autoregressive model (i.e. $AR(1)$) for $\kappa_t(i)$. Indeed, it is preferable that the time series $\kappa_t(i)$ tends towards a constant value. Therefore, the paper suggests the following dynamics for both time series :

$$\begin{cases} K_{t+1} = K_t + \mu + \sigma Z_{t+1} \\ \kappa_{t+1}(i) = \kappa_t(i) + \sigma^* Z^*_{t+1} \end{cases} \tag{8.3.1}$$

or

$$\begin{cases} K_{t+1} = K_t + \mu + \sigma Z_{t+1} \\ \kappa_{t+1}(i) = c_0 + c_1\kappa_t(i) + \sigma^* Z^*_{t+1} \end{cases} \tag{8.3.2}$$

where μ, σ, c_0, c_1 and σ^* are 5 constants. Also $Z_{t+1} \sim \mathcal{N}(0,1)$ and $Z^*_{t+1} \sim \mathcal{N}(0,1)$.
For the sake of simplicity, we consider that the two time series K_t and $\kappa_t(i)$ are independent of each other. Indeed, by observing Figure 8.2.1, a possible correlation between K_t and $\kappa_t(i)$ is not obvious. Moreover, this will simplify the calibration of the projection models with jump effects developed in the previous chapters.

To see the impact of Covid-19 on the Li & Lee model, we follow the same strategy as before. We calibrate the two time series on 2 different time periods, namely $1980 \to 2019$ and $1980 \to 2020$. The calibration is performed by using or adapting the proposition 4.1.1. In Appendix G we show the AIC, the BIC and the optimal values obtained for K_t and for $\kappa_t(i)$ with the two possible projection methods we consider. We can see that in this appendix, the year 2020 has the effect of increasing the parameter μ and σ when we take the year 2020 into the calibration time period for K_t. Concerning the $\kappa_t(i)$ time series, we can see that the RW projection method gives a better result for the AIC and the BIC for both time periods[3]. Moreover, the impact of the year 2020 on $\kappa_t(i)$ for the RW projection method is very small.

In Table 8.3.1 and 8.3.2, we displayed the values obtained for the life expectancies and single premiums for a life annuity for the calibration time period $1980 \to 2019$ and $1980 \to 2020$ by using the RWD projection method for K_t and the RW projection method for κ_t.

[3]Note that the AIC obtained with the AR(1) projection method for the $1980 \to 2019$ calibration time period is lower than the one obtained for the RW projection method However, the BIC value for the same calibration period is much lower for the RW projection method than for the AR(1) method.

Calibration time period: 1980 → 2019

Age	2020	2030	2040	2050
20	**61.67** [61.34 ; 62.01]	**63.15** [62.05 ; 64.15]	**64.53** [63.16 ; 65.83]	**65.78** [64.19 ; 67.16]
40	**42.21** [41.87 ; 42.55]	**43.60** [42.49 ; 44.62]	**44.91** [43.52 ; 46.18]	**46.09** [44.50 ; 47.46]
60	**23.91** [23.58 ; 24.24]	**25.09** [24.03 ; 26.04]	**26.20** [24.92 ; 27.40]	**27.22** [25.72 ; 28.48]
80	**8.69** [8.58 ; 8.80]	**9.26** [8.90 ; 9.61]	**9.81** [9.32 ; 10.30]	**10.34** [9.75 ; 10.89]

Calibration time period: 1980 → 2020

Age	2020	2030	2040	2050
20	**60.71**	**62.48** [61.32 ; 63.60]	**63.74** [62.17 ; 65.21]	**64.94** [63.23 ; 66.56]
40	**41.23**	**42.96** [41.76 ; 44.03]	**44.15** [42.58 ; 45.61]	**45.28** [43.58 ; 46.88]
60	**22.90**	**24.51** [23.34 ; 25.53]	**25.51** [23.97 ; 26.91]	**26.48** [24.79 ; 27.96]
80	**8.15**	**8.96** [8.56 ; 9.37]	**9.45** [8.90 ; 10.01]	**9.93** [9.27 ; 10.6]

Table 8.3.1: Life expectancies calculated using the Li & Lee model. For the calibration time period 1980 → 2020, life expectancies for the year 2020 are calculated using mortality rates observed during the year.

Calibration time period: 1980 → 2019

Year	Single premium
2020	**16.04** [15.84 ; 16.23]
2030	**16.78** [16.16 ; 17.36]
2040	**17.48** [16.71 ; 18.19]
2050	**18.12** [17.24 ; 18.86]

Calibration time period: 1980 → 2020

Year	Single premium
2020	**15.35**
2030	**16.41** [15.71 ; 17.03]
2040	**17.05** [16.15 ; 17.88]
2050	**17.65** [16.68 ; 18.54]

Table 8.3.2: Single premium for a life annuity calculated using the Li & Lee model. For the calibration time period 1980 → 2020, single premiums for the year 2020 are calculated using mortality rates observed during the year.

We can observe in Table 8.3.1 that if we take a person aged 20 in 2050, we can see that Covid-19 causes a decrease of about one year in life expectancy. In the Lee-Carter model, we saw that the decrease was about two years in 2050 (see Table 4.2.1). Also, the results obtained with the Li & Lee model are very close to those obtained with the Lee-Carter model with the basic projection method. For example, the life expectancy in 2050 for a person aged 20 was 66.37 for the calibration time period 1980 $\rightarrow$ 2019 and 64.33 for the calibration time period 1980 $\rightarrow$ 2020.
Concerning the single premiums for life annuities, the same observations can be made as those seen with the Lee-Carter model.

8.4 Projection with jump effects.

In addition to the projection models recommended by the author, we also implemented the following models for K_t and $\kappa_t(i)$:

- Projection with permanent jump effects with $Y \sim \mathcal{N}(m, s^2)$.
- Projection with permanent jump effects with $Y \sim \mathcal{E}\text{xp}(\lambda)$.
- Projection with transitory jump effects with $Y \sim \mathcal{N}(m, s^2)$.
- Projection with transitory jump effects with $Y \sim \mathcal{E}\text{xp}(\lambda)$.

However, for $\kappa_t(i)$, we only incorporate these models on the random walk without drift, i.e.

$$\kappa_{t+1}(i) = \kappa_t(i) - p\ \mathbb{E}[Y] + \sigma^* Z^*_{t+1} + Y_{t+1} N_{t+1} \tag{8.4.1}$$
$$\kappa_{t+1}(i) = \kappa_t(i) + \sigma^* Z^*_{t+1} + Y_{t+1} N_{t+1} - Y_t N_t \tag{8.4.2}$$

where $\mathbb{E}[Y]$ is the expectation value of Y, equation (8.4.1) is for the permanent jump effects model and equation (8.4.2) is for the transitory jump effects model.

The reason why we only incorporate jumps in the RW model and not in the AR(1) model is that with RW, we can directly use the propositions 6.1.1, 6.1.3, 7.1.1 and 7.1.5 for the calibration of the projection model by simply positing $\mu = 0$. However for AR(1), we have to adapt and redevelop these propositions because of the constant c_1 multiplying $\kappa_t(i)$. This can lead to some work without the certainty of having a real difference between RW and AR(1) when we incorporate jumps on both projection models.

Once again, we calibrate these different projection methods with jump effects over the two calibration time periods 1980 $\rightarrow$ 2019 and 1980 $\rightarrow$ 2020. The values obtained for the AIC and BIC are presented in Appendix G (see Table 10.7.4 and 10.7.5). We can see that none of the projection models with jump effects have a lower value for AIC and BIC than those obtained previously with a projection method without jump.

In conclusion, the incorporation of jumps in the projection of the Li & Lee model does not increase the quality of the fit when we take the year 2020 into the calibration time period. This statement is contrary to the one obtained with the Lee-Carter model where the incorporation of jumps increases considerably the quality of the calibration[4].

[4]For the calibration time period with the year 2020, we obtained a lower value for the AIC and BIC and we considered permanent or transitory jumps into the projection method.

Chapter 9

Conclusion.

In this dissertation, we have seen that the pandemic caused by Covid-19 resulted in a significant excess of mortality for the Belgian population in the year 2020. The pandemic mainly affected the elderly, while the lockdown put in place to face this pandemic caused a decrease in mortality among the younger population. Much of this dissertation has dealt with the impact of this pandemic on a mortality model such as the Lee-Carter model. More specifically, the effect on the projection of the mortality factor κ_t. We studied different projection methods such as the basic projection method (i.e. random walk with drift), a method we called "deformation of the curve" and finally another method with permanent jump effects and transitory jump effects with two different distributions for the jump variable.

We have seen that the basic projection method has greatly impacted by the year 2020. Furthermore, it was not possible to produce future pandemics or mortality shocks with this projection method. The "deformation of the curve" method allowed us to easily add mortality shocks without changing the dynamics of the mortality factor. This was a great advantage as one can still use the basic projection method which has proven to be very effective in the past. However, the disadvantage was that the method only simulated mortality shocks with the same characteristics as the shock created by Covid-19 (i.e. the same age distribution for excess mortality). The projection method with permanent and transitory jumps allowed us to simulate random jumps into the time series. The transitory jumps completely mitigated the effect of Covid-19 while the permanent jumps was a compromise between the basic projection method and the transitory jumps model. Regarding the distribution of the jump variable, we have seen that it weakly affects the quality of the calibration, but the exponential distribution had the advantage of creating only positive jumps and of having to optimise only one parameter for the jump variable (instead of two for the normal distribution). Finally, for all the projection methods described above, we calculated the life expectancies and single premiums of a life annuity for different periods and compared them with each other.

In the last chapter, we also studied the impact of Covid-19 through a multi-population model (i.e. the Li & Lee model). We took the combined Belgian and Dutch population as the reference population and found that the impact of Covid-19 was less severe when considering the multi-population model. The consequence of this observation was that projection models with jump did not increase the quality of the calibration of the time series.

To conclude, we can say that Covid-19 was a major event that severely affected our classical projection model. However, we have seen how we can mitigate the impact of Covid-19 with different models and how we can use this event to produce future mortality shocks. One way to improve our projection models would be to remove the assumption that a pandemic (or mortality shock) would last only one year. Indeed, for pandemics, it is not uncommon to have resurgences and waves in subsequent years. One could therefore consider a model that takes this observation into account by allowing the probability of occurrence of a pandemic to vary according to what has happened in previous years.

Chapter 10

Appendix.

10.1 Appendix A.

We divide the age group $0 \rightarrow 99$ into 5 subgroups $\mathbf{(0 \rightarrow 19\ ;\ 20 \rightarrow 39\ ;\ 40 \rightarrow 64\ ;\ 65 \rightarrow 84\ ;\ 85 \rightarrow 99)}$.

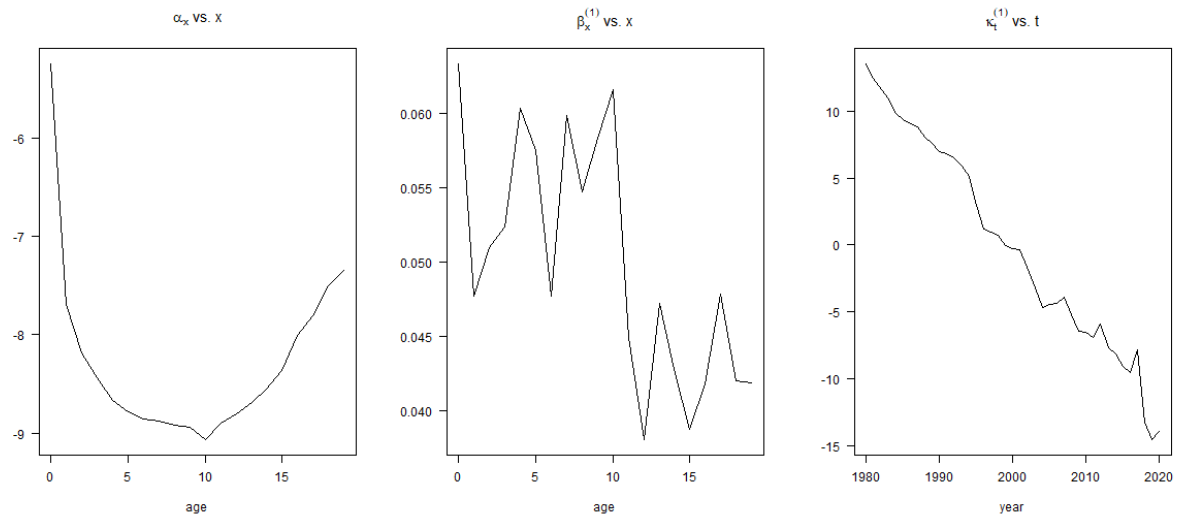

Figure 10.1.1: Calibration of the Lee-Carter model for the Belgian population and for the subgroup: $0 \rightarrow 19$.

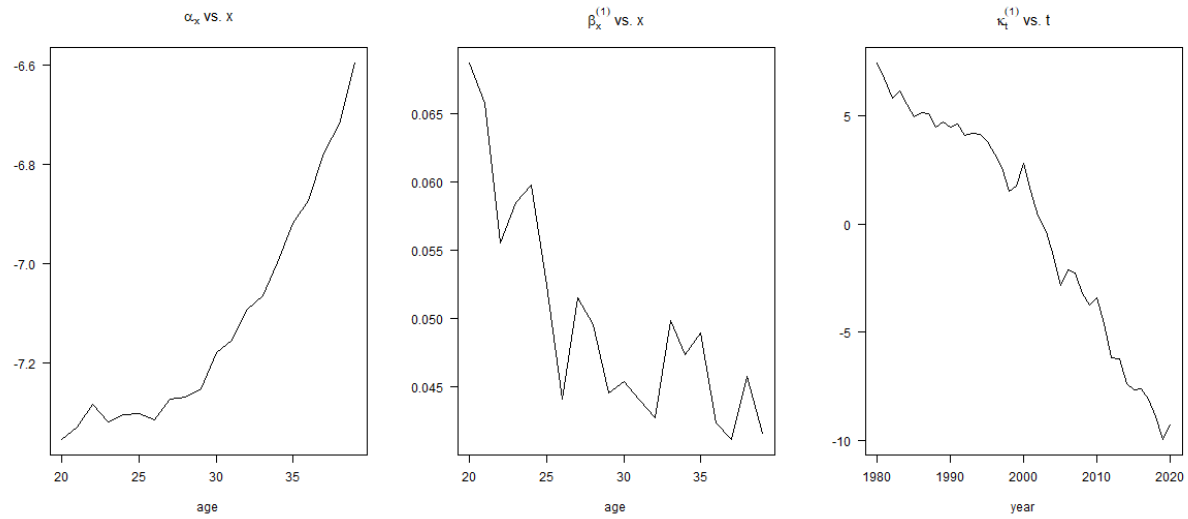

Figure 10.1.2: Calibration of the Lee-Carter model for the Belgian population and for the subgroup: $20 \rightarrow 39$.

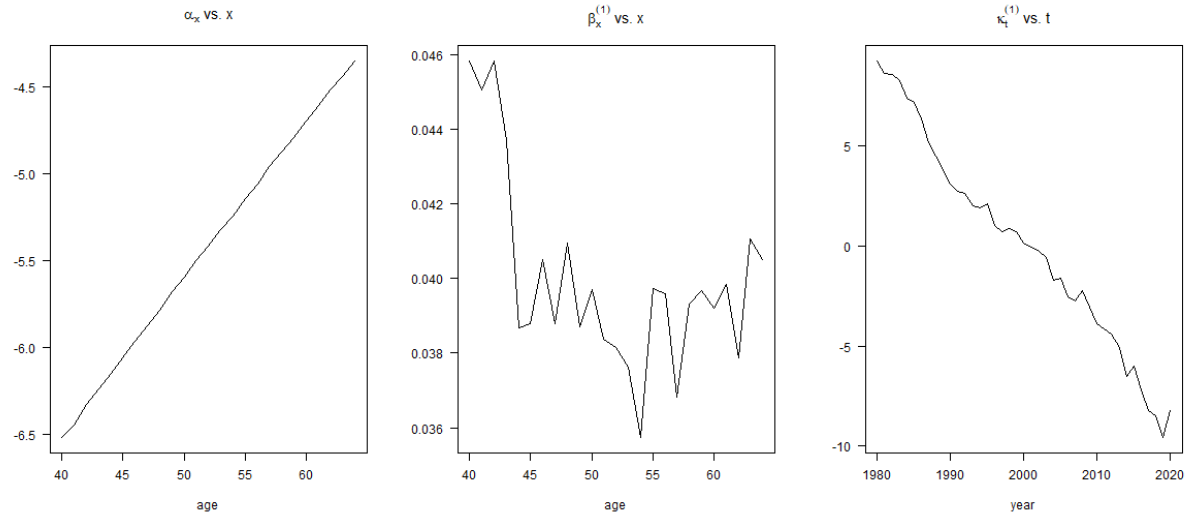

Figure 10.1.3: Calibration of the Lee-Carter model for the Belgian population and for the sub-group: $40 \rightarrow 64$.

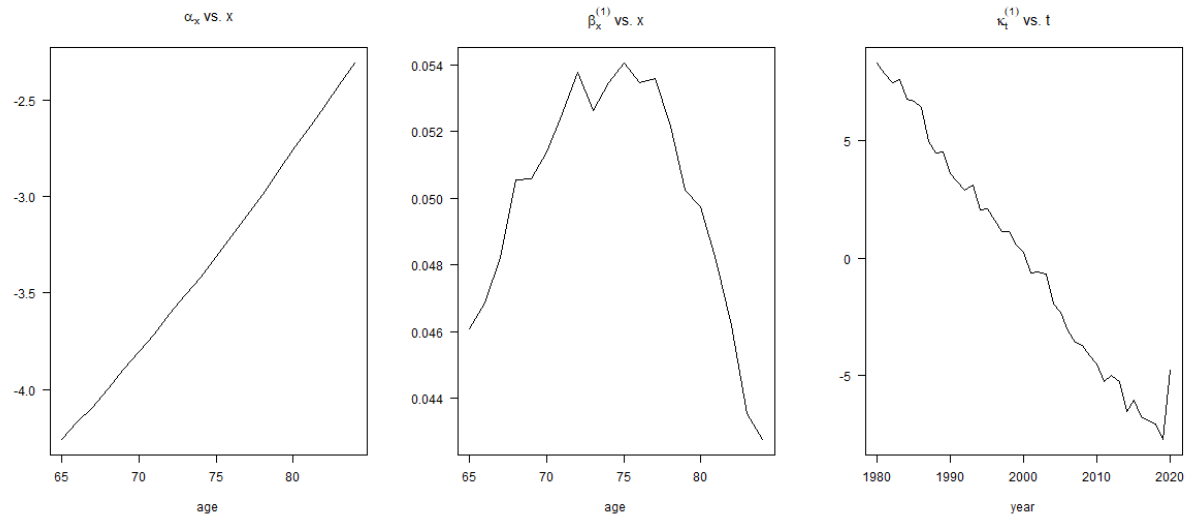

Figure 10.1.4: Calibration of the Lee-Carter model for the Belgian population and for the subgroup: $65 \rightarrow 84$.

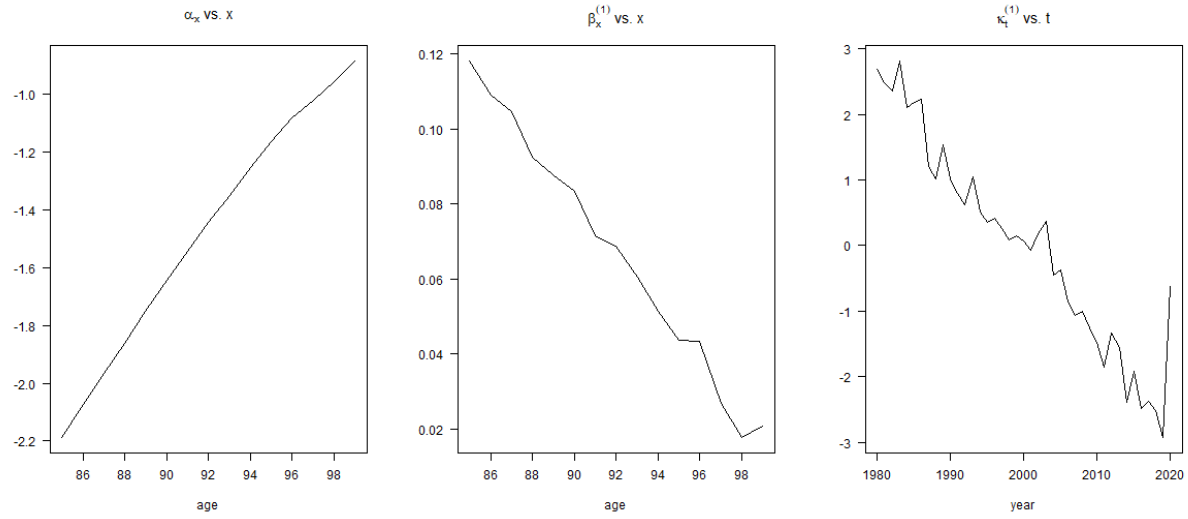

Figure 10.1.5: Calibration of the Lee-Carter model for the Belgian population and for the subgroup: $85 \rightarrow 99$.

10.2 Appendix B.

Stochastic Mortality Modeling

Documentation of the R-shiny app: GAPC

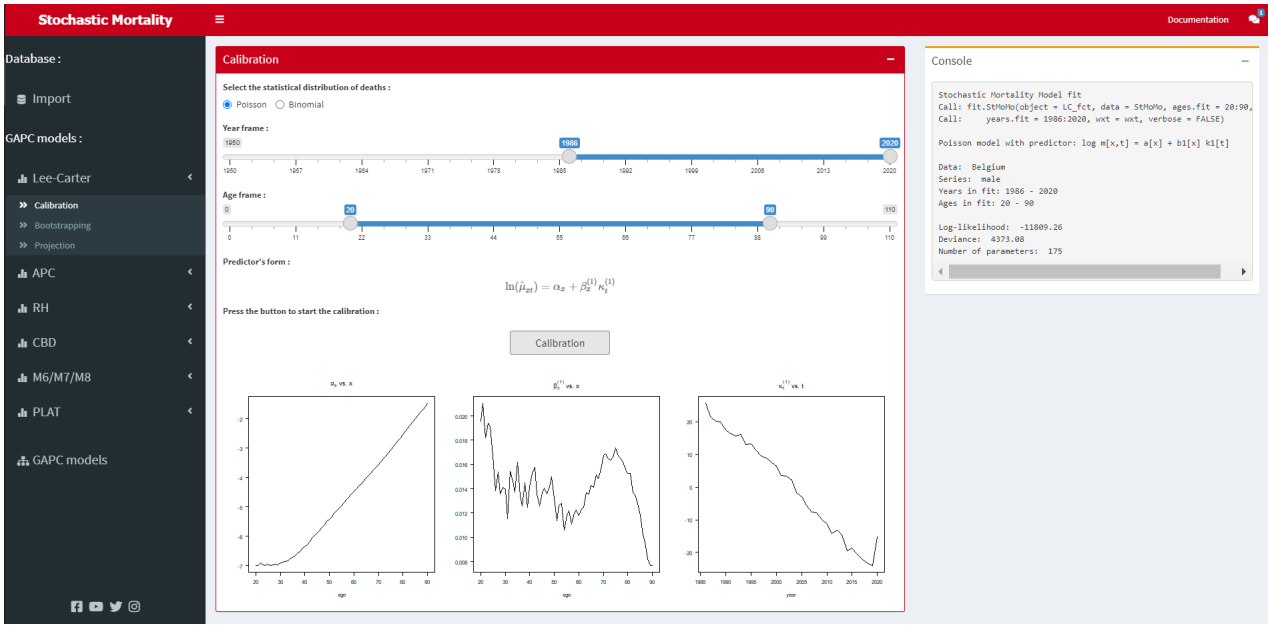

Author: Cédric Turcksin
Contact: cedric.turcksin@hotmail.com

Introduction

The purpose of this document is to quickly explain how the R-shiny application works and some of the main features present in the application. The main objective of the application is to provide an intuitive way to work with the R package StMoMo. The application allows the user to quickly calibrate and simulate one-year mortality rates/death probabilities with various generalized age-period-cohort (GAPC) models available in this package. The following document does not explain in detail each algorithm present in the application but rather how to use the application effectively. For more details on how to use some of the functions of the StMoMo package, please consult the StMoMo package documentation available here[1].
In the following section, we will first discuss the general aspect of the application, and then we will detail each section of the application one by one.

General aspect

The application can be started by opening and executing the R file app-GAPC.R in the folder "TOOL"[2]. A recent version of R is required (the app was developed under the version 4.0.4) and the following packages must be installed :

- shiny
- shinydashboard
- dashboardthemes
- shinycssloaders
- demography
- StMoMo
- fanplot
- collapsibleTree
- sfsmisc
- forecast

We recommend that you select the "Run External" option (for RStudio users only) available by clicking on the small down arrow next to the "Run App" button. Once the application is launched, a new tab in your default web browser will open and display the application (Figure 10.2.1).

[1] https://cran.r-project.org/web/packages/StMoMo/vignettes/StMoMoVignette.pdf
[2] We invite the user to not move files outside the folder!

In the Figure 10.2.1, the sidebar is on the left and allows the user to navigate through different sections. The app is composed of two main sections :

- ☐ Database
- ☐ GAPC models

The Database section allows the user to import the chosen database and the GAPC Models section allows the user to choose a particular stochastic mortality model to use on the selected database.
The "GAPC Models" section presents the classification of the different GAPC models in the form of an interactive retractable tree (Figure 10.2.2).
At the top right, the "Documentation" box directs the user to the documentation of the R-package StMoMo.

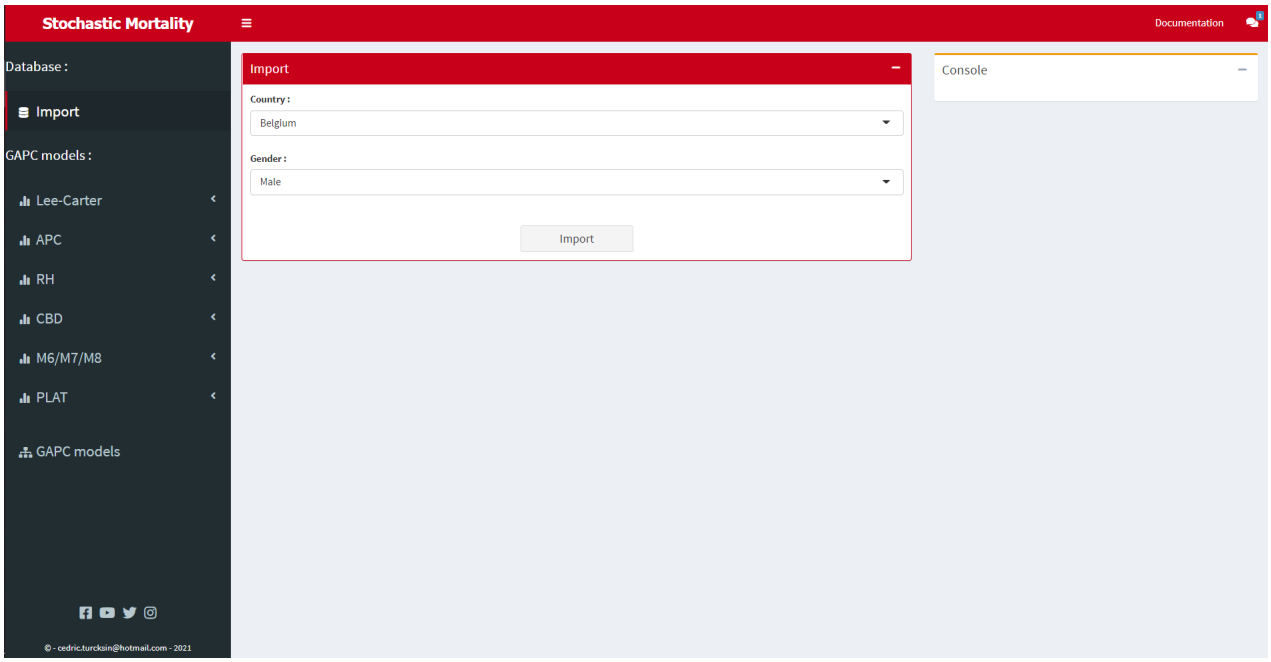

Figure 10.2.1: Overview of the application.

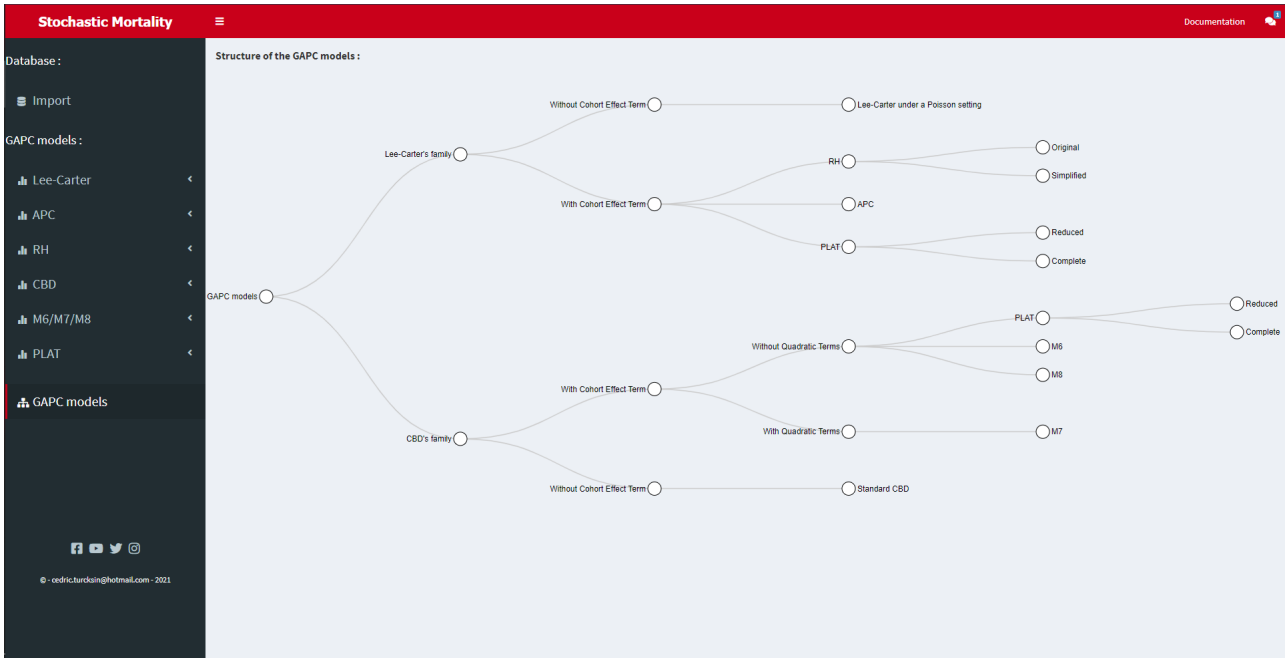

Figure 10.2.2: The GAPC models section.

Import

The first step is to select the desired database. To achieve this, the user selects the import section from the sidebar (as in Figure 10.2.1). Then, in the Import tab, the user selects the appropriate country and gender of interest. After this, the user presses the "Import" button and after a moment, a text is displayed in the Console tab showing some information about the database. If the user wishes to select another country or gender at a later stage, he simply selects the new country or gender and press the "Import" button again. There is no need to restart the application.

A few words about the database. To calibrate a GAPC model, the application needs two different tables. One is a table containing the number of deaths and the other contains the risk exposure by age and year. Some countries are present in the application but the user may be interested in adding his own database. To do this, the user simply places the desired database in the "Other" folder of the "Database" folder. The user can place the two tables containing the number of deaths and the risk exposure there. We invite the user to make sure that his table is compatible with the application by looking at a database already present in the application to avoid format errors. Indeed, the tables must be in ".txt" format and with "tab" as column separator (Figure 10.2.3).

The last thing to do is to put the file name of the two tables in the app-GAPC.R file on lines 2 and 3.

Year	Age	Female	Male	Total
1950	0	3307.13	4479.54	7786.67
1950	1	206.00	274.03	480.03
1950	2	106.00	152.02	258.02
1950	3	84.00	117.02	201.02
1950	4	55.00	71.00	126.00
1950	5	39.00	47.00	86.00
1950	6	29.00	43.00	72.00
1950	7	30.00	37.00	67.00
1950	8	18.00	25.00	43.00
1950	9	26.00	34.00	60.00
1950	10	28.00	42.00	70.00

Figure 10.2.3: Example of a table containing the number of deaths respecting the required format.

GAPC models

Once the import phase is done, the user can use various GAPC model present in the StMoMo package :

- Lee-Carter model under a Poisson setting
- APC model
- Renshaw and Haberman model
- CBD model
- M6/M7/M8 model
- Plat model

The user then needs to click on the GAPC model of his choice in the sidebar and three new subsections will appear: Calibration, Bootstrapping and Projection (Figure 10.2.4). Each sub-section will be detailed in the following.

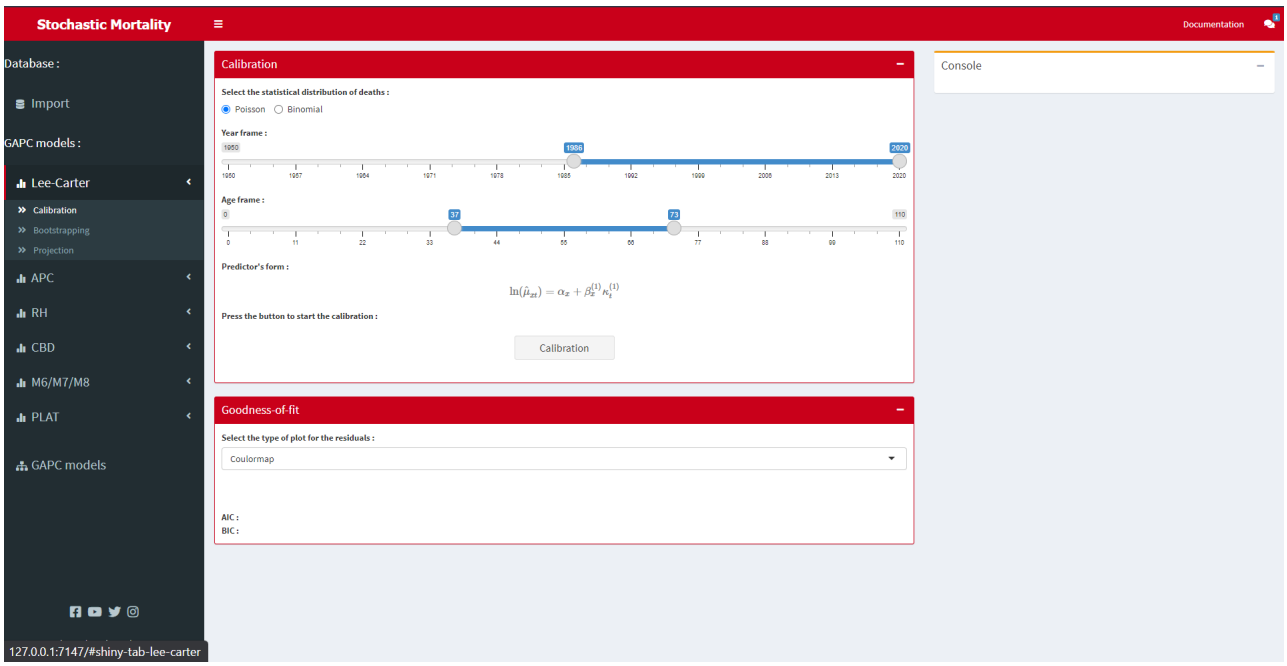

Figure 10.2.4: The three new subsections after the user clicks on the Lee-Carter model.

Calibration

This subsection is composed of 3 different tabs :

- Calibration
- Goodness-of-fit
- Console

In the Calibration tab, the user can select the statistical distribution of deaths, the year and the age frame. If the user chooses the Poisson distribution, then the calibration targets the force of mortality μ_{xt}. On the other hand, if he chooses the Binomial distribution then the calibration targets the one-year death probabilities q_{xt}.

Once the user has selected the desired options, he can press the "Calibration" button. The calibration is performed with the function *fit.StMoMo(.)* and the parameters of the GAPC model appear below the button. In addition, some information about the calibration is displayed in the Console tab and in the Goodness-of-fit tab as we can see in Figure 10.2.5.

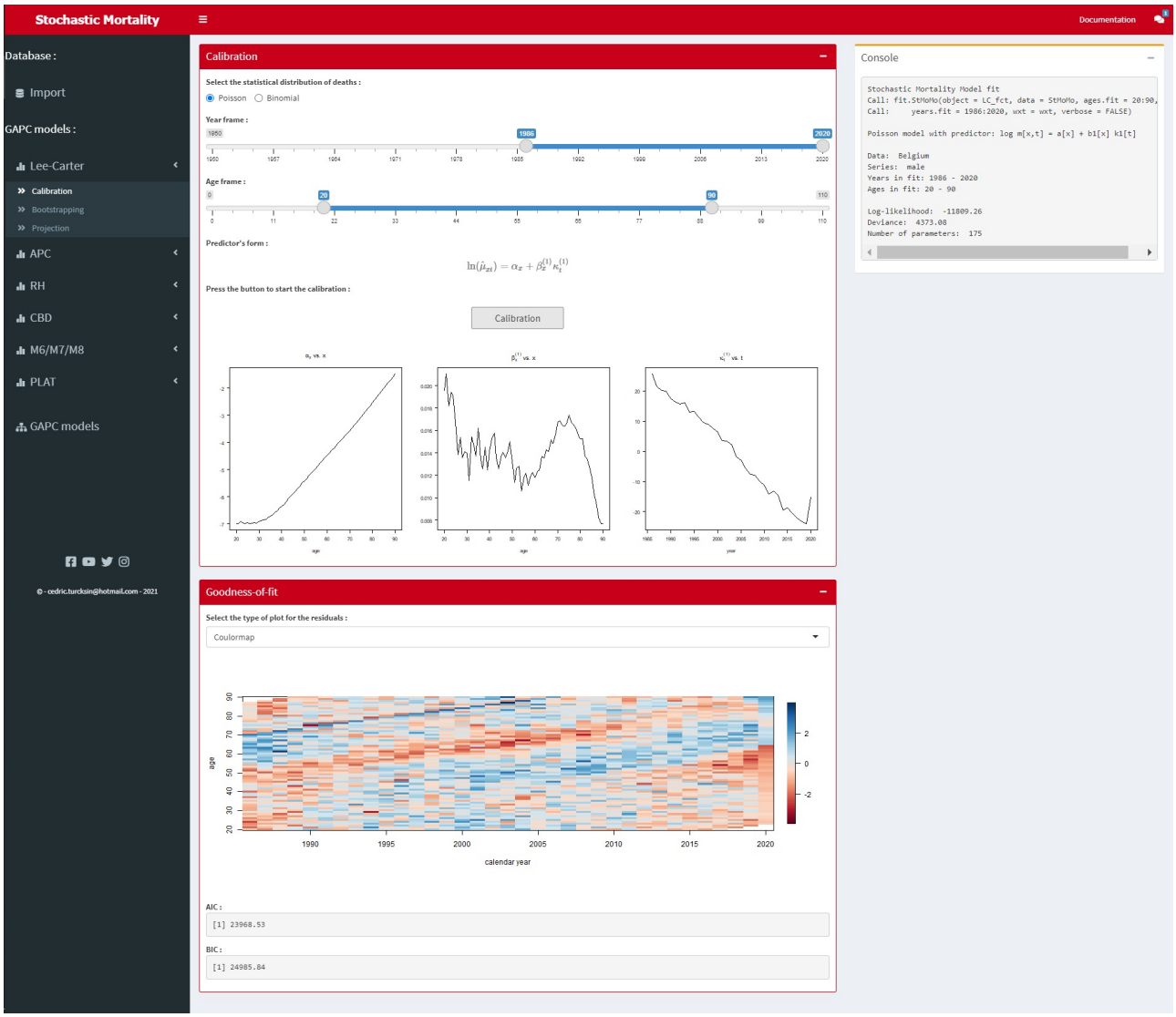

Figure 10.2.5: The Calibration subsection for the Lee-Carter model.

Bootstrapping

Two tabs are present in this section: Parameter uncertainty and Console. In the Parameter uncertainty tab, the user can select the bootstrap method and the number of bootstrap samples to produce. Then, by pressing the "Bootstrapping" button, the parameter uncertainty associated with each parameter of the selected GAPC model is displayed below the button (Figure 10.2.6).

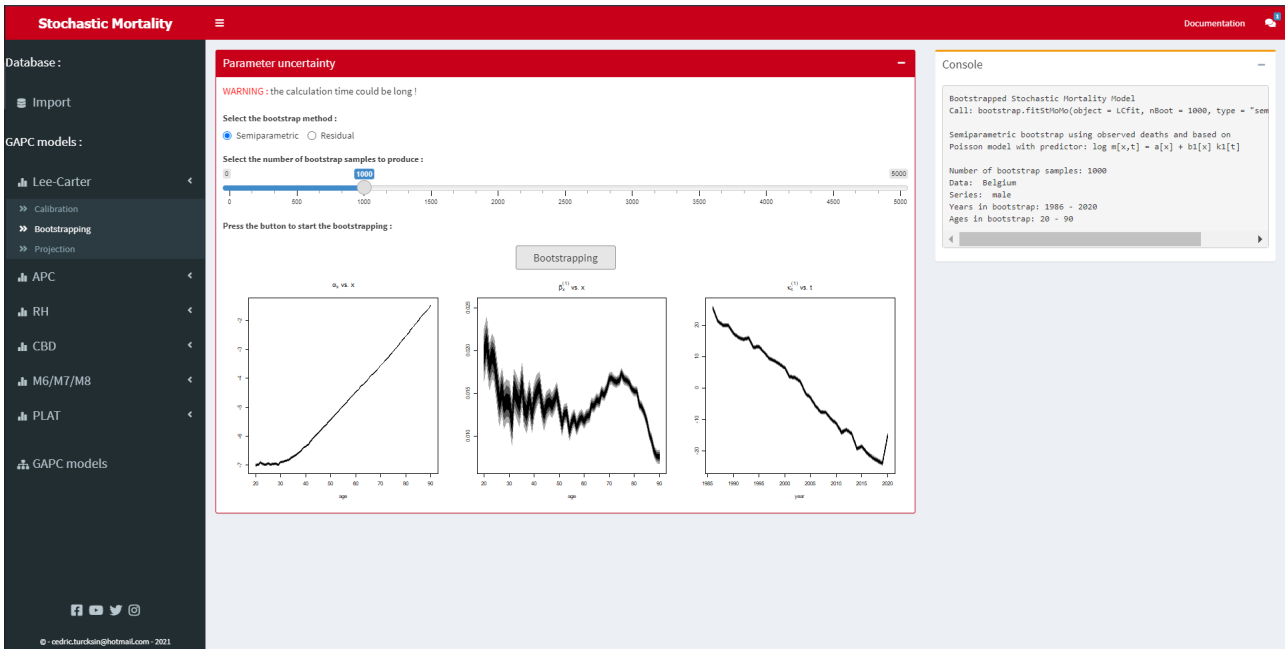

Figure 10.2.6: The Bootstrapping subsection.

The bootstrapping procedure is done with the function *bootstrap.fitStMoMo(.)*. As this procedure can be time-consuming, it is possible to skip this step and go directly to the next subsection.

Projection

The last subsection is composed of 5 different tabs :

- Projection
- Mortality rates
- Life expectancies
- Console
- Download

In the Projection tab, the user must choose 5 different options for the projection. The first one is the method of projection for the time-dependent parameters: MRWD[3] or ARIMA. If the ARIMA method is selected, the estimation and forecasting of the ARIMA processes is done with the function *Arima(.)* and *auto.arima(.)* from the R-package Forecast.

[3]MRWD stands for multivariate random walk with drift

The second option concerns the jump-off rates, i.e. the rates from the final year of observation (the observed one or the fitted one) to be used in the projection of mortality rates. The third one allows the user to set or not the *seed* before simulating the time series. The last 2 tabs allow the user to choose the maximum projection year and the number of simulations. Once the appropriate options have been selected, the user can press the "Projection" button and the projected time-dependent parameters of the GAPC model are displayed below along with some information about the projection in the Console tab (Figure 10.2.7).

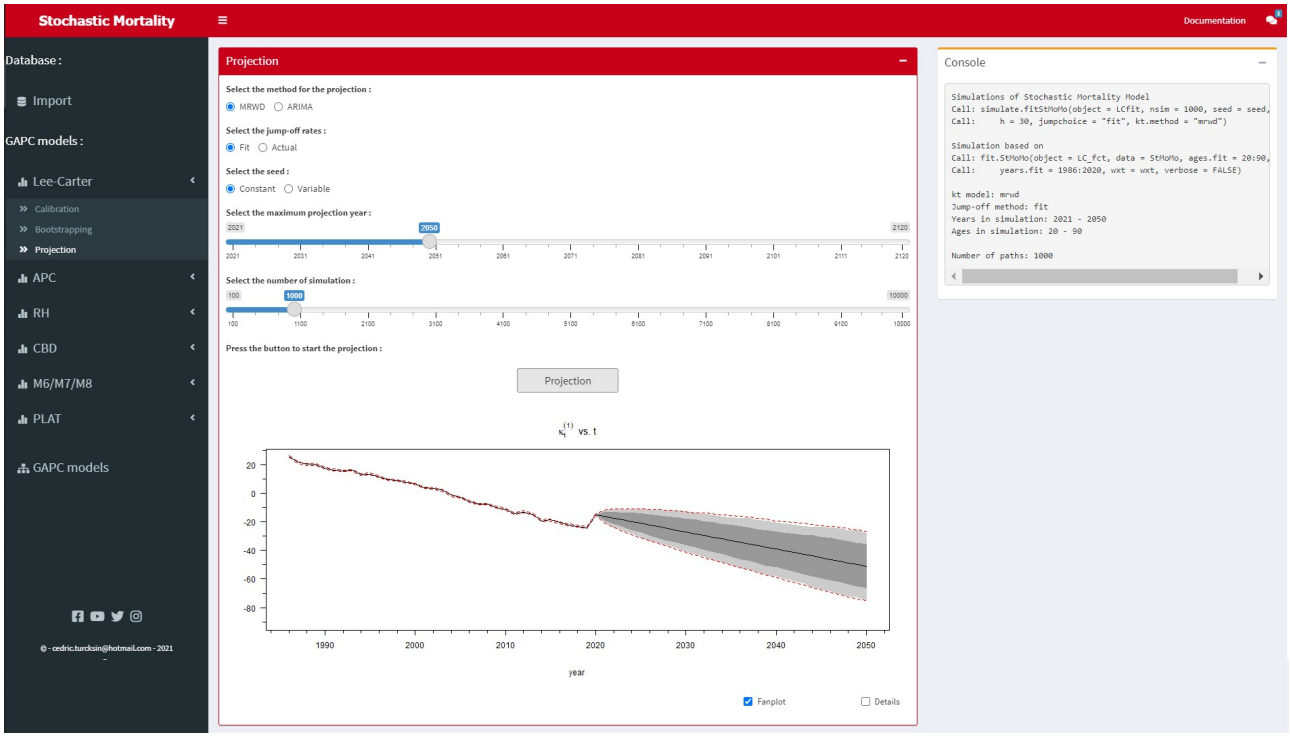

Figure 10.2.7: The Projection subsection with the Projection tab and the Console tab.

The black line in the plot in Figure 10.2.7 represents the central forecast. The dark grey corresponds to a confidence interval of 80% and the light grey a confidence interval of 95%. If the bootstrapping step has been done, the red dotted line corresponds to a confidence interval of 95% taking into account the uncertainty of the parameters.
Two small check boxes are present at the bottom of the tab. The "Fanplot" is always selected and displays the graph with the confidence interval. If the box is unchecked, it displays some simulated trajectories of the time-dependent parameters of the GAPC model. The "Details" check box shows some details about the legend of the graph.

After pressing the "Projection" button, the fitted and projected mortality rates and life expectancies appear in the tabs Mortality rates and Life expectancies (Figure 10.2.8 and Figure 10.2.9).

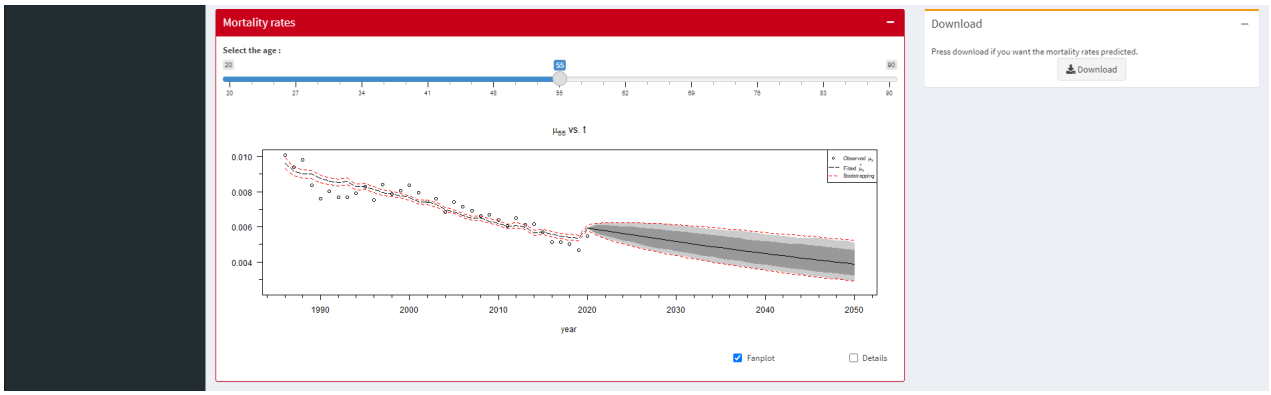

Figure 10.2.8: The Mortality rates tab and the Download tab.

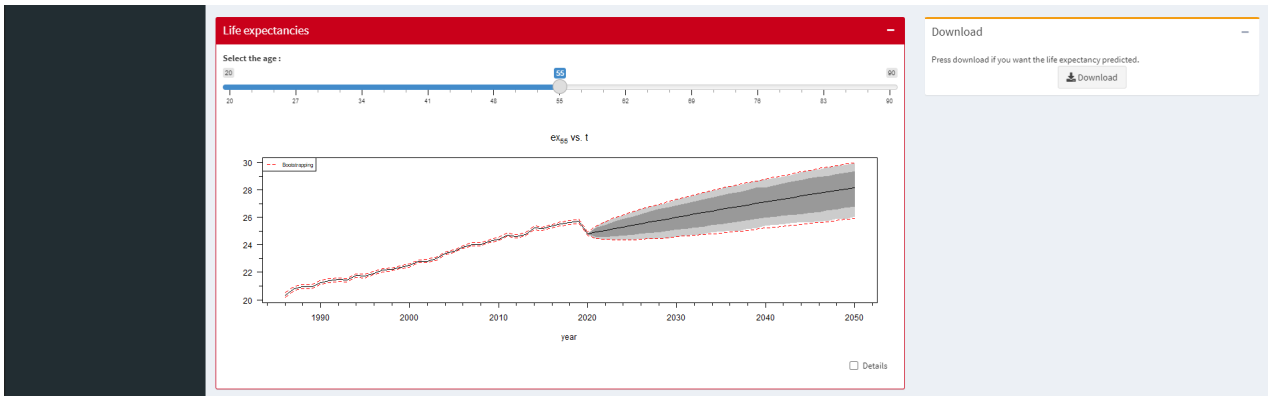

Figure 10.2.9: The Life expectancies tab and the Download tab.

Life expectancies are calculated vertically, which means that the life expectancies for a particular year n are calculated by taking only the mortality rates for that particular year n.

A feature available only for the Mortality rates tab and Life expectancies tab is hidden in the "details" check box. Once the box is checked, a box appears below the graph with information about the legend and the possibility of obtaining the exact value of the mortality rate or life expectancy of a particular year (Figure 10.2.10).

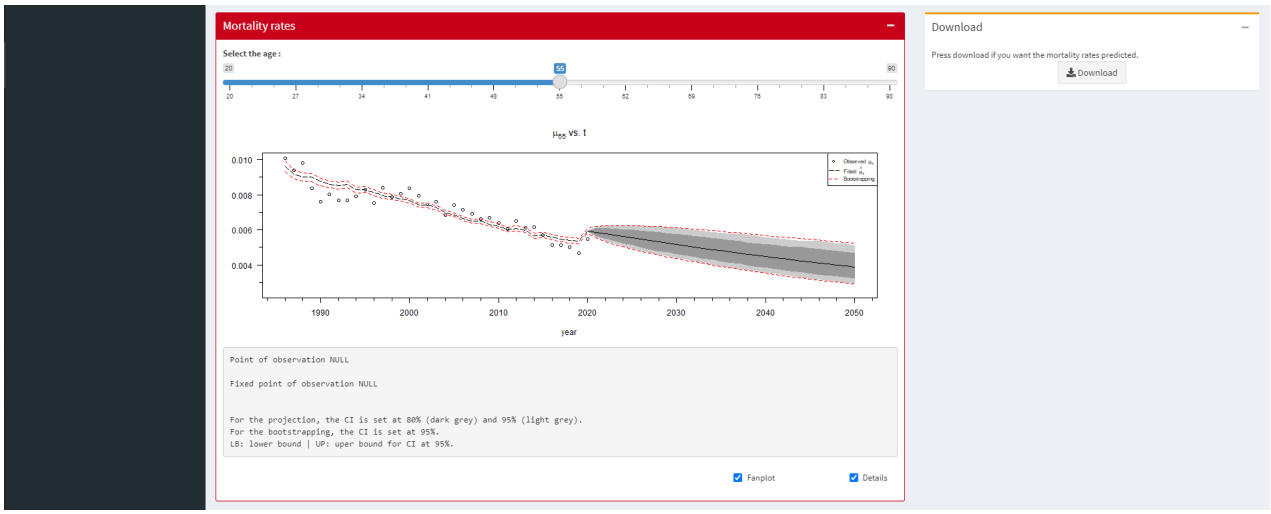

Figure 10.2.10: The Mortality rates tab with the "details" check box open.

If the user moves the mouse pointer in the graph, the value of the fitted and observed mortality rate for the particular year where the mouse pointer is located is displayed. These values are displayed under "Observation point". If the user clicks on a particular point in the graph, the fitted and observed mortality rate values are displayed under "Fixed observation point".

The last thing to note is that the application allows the user to download the mortality rates and life expectancies obtained with the application. A CSV file is obtained with the following columns:

- Year
- Age
- mx_central
- mx_lower_2.5
- mx_lower_10
- mx_upper_90
- mx_upper_97.5
- mx_lower_BOO_2.5
- mx_upper_BOO_97.5

The mx_central corresponds to the fitted mortality rates and the central forecast. The mx_lower_2.5 and mx_lower_10 are the lower bound for a confidence interval equal to 95% and 80% respectively. These values are only present for projected years and not for the years present in the calibration step. The mx_upper_90 and mx_upper_97.5 are the same but this time for the upper bound. If the bootstrapping step has been performed, the columns mx_lower_BOO_2.5 and mx_lower_BOO_97.5 appear for the fitted and projected mortality rates. Theses 2 columns corresponds to the lower and upper bound of the parameter uncertainty with a confidence interval of 95%.

If you have any further questions, please do not hesitate to contact the author of the application at : cedric.turcksin@hotmail.com

10.3 Appendix C.

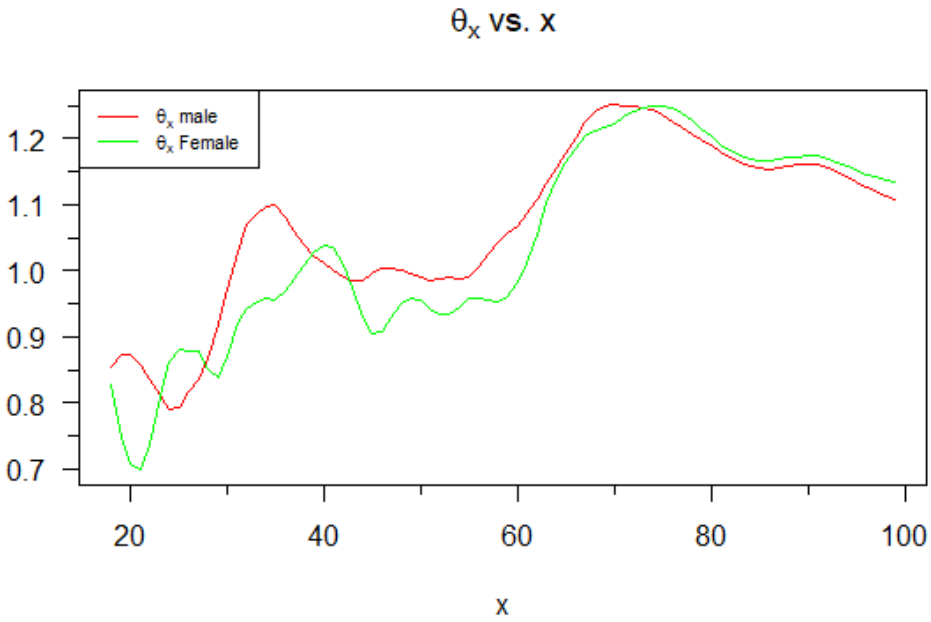

Figure 10.3.1: The process θ_x smoothed for the Belgian male population in red and female population in green.

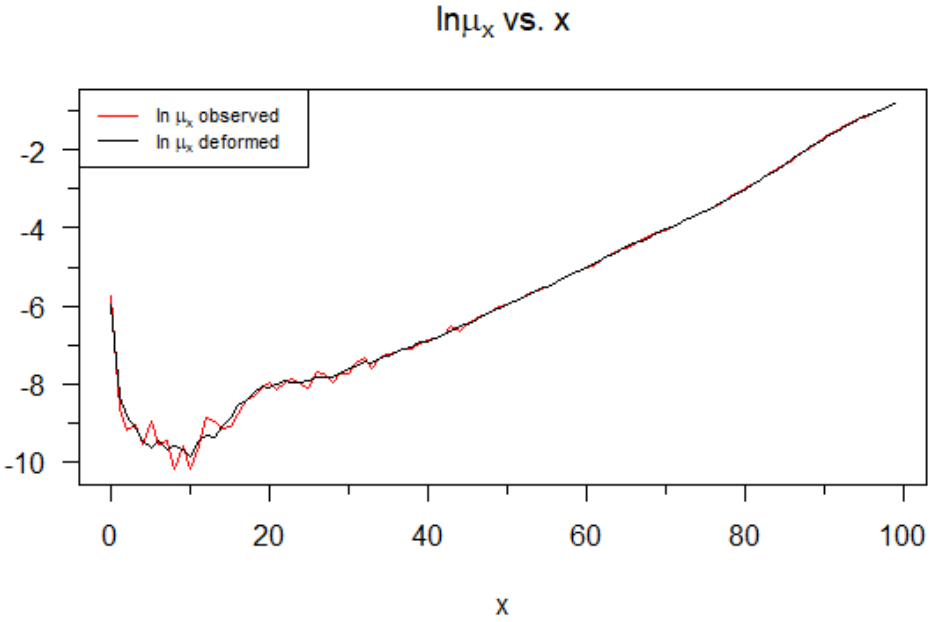

Figure 10.3.2: $\ln \mu_{x,2020}$(observed) in red and $\ln \mu_{x,2020}$(deformed) in black for the Belgian population.

Calibration time period: 1980 → 2019

Age	2020	2030	2040	2050
20	**60.71** [60.35 ; 61.06]	**63.35** [61.91 ; 64.53]	**64.88** [63.27 ; 66.31]	**66.27** [64.55 ; 67.86]
40	**41.23** [40.89 ; 41.56]	**43.83** [42.38 ; 44.96]	**45.28** [43.71 ; 46.66]	**46.61** [44.93 ; 48.14]
60	**22.89** [22.59 ; 23.19]	**25.38** [23.91 ; 26.39]	**26.65** [25.16 ; 27.87]	**27.81** [26.28 ; 29.16]
80	**8.16** [8.01 ; 8.30]	**9.54** [8.67 ; 10.09]	**10.22** [9.33 ; 10.90]	**10.86** [9.95 ; 11.64]

Table 10.3.1: Life expectancies calculated with the model for $p = 10\%$.

Calibration time period: 1980 → 2019

Year	Single premium
2020	**15.35** [15.15 ; 15.54]
2030	**16.97** [16.00 ; 17.61]
2040	**17.77** [16.80 ; 18.53]
2050	**18.49** [17.51 ; 19.32]

Table 10.3.2: Single premiums calculated with the model for $p = 10\%$.

10.4 Appendix D.

Result of the calibration with the parameter p left free.

Time period	μ	σ	p	m	s
1980 - 2019	-2.0740	0.7056	0.7557	-0.7525	2.4194
1980 - 2020	-1.6603	2.2234	0.0249	17.4611	0.0033

Time period	AIC	BIC
1980 - 2019	181.29	189.61
1980 - 2020	196.80	205.25

Table 10.4.1: Optimal parameters, AIC and BIC for the model with permanent jump effects and $Y \sim \mathcal{N}(m, s^2)$.

Time period	μ	σ	p	λ
1980 - 2019	-2.0739	2.2416	2.06e-05	5.0522
1980 - 2020	-1.6611	2.2318	0.0411	0.0867

Time period	AIC	BIC
1980 - 2019	181.64	188.30
1980 - 2020	198.23	204.99

Table 10.4.2: Optimal parameters, AIC and BIC for the model with permanent jump effects and $Y \sim \mathcal{E}xp\,(\lambda)$.

Life expectancy and life annuity.

Calibration time period: 1980 → 2020

Age	2020	2030	2040	2050
20	**60.71**	**61.86** [59.83 ; 63.21]	**63.23** [60.54 ; 65.01]	**64.48** [61.43 ; 66.62]
40	**41.23**	**42.43** [40.52 ; 43.70]	**43.72** [41.18 ; 45.41]	**44.91** [42.02 ; 46.94]
60	**22.90**	**24.18** [22.54 ; 25.27]	**25.29** [23.11 ; 26.76]	**26.32** [23.83 ; 28.09]
80	**8.15**	**8.92** [8.09 ; 9.48]	**9.49** [8.37 ; 10.27]	**10.04** [8.74 ; 11.00]

Table 10.4.3: Life expectancies calculated with the model with permanent jump effects and $Y \sim \mathcal{N}(m, s^2)$. Life expectancies for the year 2020 are calculated using mortality rates observed during the year.

Calibration time period: 1980 → 2020

Age	2020	2030	2040	2050
20	**60.71**	**61.94** [59.74 ; 63.23]	**63.33** [60.14 ; 65.19]	**64.64** [61.00 ; 66.74]
40	**41.23**	**42.51** [40.43 ; 43.72]	**43.82** [40.81 ; 45.58]	**45.06** [41.61 ; 47.06]
60	**22.90**	**24.25** [22.47 ; 25.30]	**25.38** [22.79 ; 26.90]	**26.46** [23.48 ; 28.19]
80	**8.15**	**8.95** [8.05 ; 9.49]	**9.54** [8.21 ; 10.35]	**10.11** [8.56 ; 11.06]

Table 10.4.4: Life expectancies calculated with the model with permanent jump effects and $Y \sim \mathcal{E}xp\,(\lambda)$. Life expectancies for the year 2020 are calculated using mortality rates observed during the year.

Calibration time period: 1980 → 2020

Year	Single premium
2020	**15.35**
2030	**16.21** [15.16 ; 16.91]
2040	**16.92** [15.53 ; 17.84]
2050	**17.56** [15.99 ; 18.66]

Table 10.4.5: Single premiums calculated with the model with permanent jump effects and $Y \sim \mathcal{N}(m, s^2)$. Single premiums for the year 2020 are calculated using mortality rates observed during the year.

Calibration time period: 1980 → 2020

Year	Single premium
2020	**15.35**
2030	**16.25** [15.11 ; 16.92]
2040	**16.97** [15.32 ; 17.93]
2050	**17.64** [15.76 ; 18.72]

Table 10.4.6: Single premiums calculated with the model with permanent jump effects and $Y \sim \mathcal{E}xp\,(\lambda)$. Single premiums for the year 2020 are calculated using mortality rates observed during the year.

10.5 Appendix E.

Result of the calibration with the parameter p left free.

Time period	μ	σ	p	m	s
1980 - 2019	-2.0735	2.2417	5.28 e-09	-0.5593	2.3378
1980 - 2020	-2.0957	2.2279	0.0163	17.4489	0.0015

Time period	AIC	BIC
1980 - 2019	183.64	191.96
1980 - 2020	197.66	206.10

Table 10.5.1: Optimal parameters, AIC and BIC for the model with transitory jump effects and $Y \sim \mathcal{N}(m, s^2)$.

Time period	μ	σ	p	λ
1980 - 2019	-2.0744	2.2412	1.00 e-09	5.8937
1980 - 2020	-2.1081	2.2478	0.0214	0.0717

Time period	AIC	BIC
1980 - 2019	181.64	188.29
1980 - 2020	199.42	206.17

Table 10.5.2: Optimal parameters, AIC and BIC for the model with transitory jump effects and $Y \sim \mathcal{E}\mathrm{xp}\,(\lambda)$.

Life expectancy and life annuity.

Calibration time period: 1980 → 2020

Age	2020	2030	2040	2050
20	**60.71**	**62.09** [60.83 ; 63.18]	**63.71** [62.10 ; 65.20]	**65.22** [63.44 ; 66.88]
40	**41.23**	**42.64** [41.46 ; 43.67]	**44.17** [42.65 ; 45.59]	**45.61** [43.92 ; 47.19]
60	**22.90**	**24.36** [23.35 ; 25.25]	**25.69** [24.37 ; 26.92]	**26.93** [25.46 ; 28.31]
80	**8.15**	**9.01** [8.49 ; 9.47]	**9.70** [9.01 ; 10.35]	**10.37** [9.58 ; 11.12]

Table 10.5.3: Life expectancies calculated with the model with transitory jump effects and $Y \sim \mathcal{N}(m, s^2)$. Life expectancies for the year 2020 are calculated using mortality rates observed during the year.

Calibration time period: 1980 → 2020

Age	2020	2030	2040	2050
20	**60.71**	**62.14** [60.93 ; 63.27]	**63.78** [62.20 ; 65.15]	**65.29** [63.34 ; 66.94]
40	**41.23**	**42.69** [41.55 ; 43.76]	**44.24** [42.74 ; 45.54]	**45.68** [43.82 ; 47.25]
60	**22.90**	**24.40** [23.42 ; 25.33]	**25.75** [24.45 ; 26.87]	**26.99** [25.39 ; 28.35]
80	**8.15**	**9.03** [8.53 ; 9.51]	**9.73** [9.05 ; 10.33]	**10.40** [9.54 ; 11.15]

Table 10.5.4: Life expectancies calculated with the model with transitory jump effects and $Y \sim \mathcal{E}\mathrm{xp}\,(\lambda)$. Life expectancies for the year 2020 are calculated using mortality rates observed during the year.

Calibration time period: 1980 → 2020

Year	Single premium
2020	**15.35**
2030	**16.33** [15.68 ; 16.90]
2040	**17.17** [16.34 ; 17.94]
2050	**17.95** [17.03 ; 18.79]

Table 10.5.5: Single premiums calculated with the model with transitory jump effects and $Y \sim \mathcal{N}(m, s^2)$. Single premiums for the year 2020 are calculated using mortality rates observed during the year.

Calibration time period: 1980 → 2020

Year	Single premium
2020	**15.35**
2030	**16.35** [15.73 ; 16.94]
2040	**17.21** [16.39 ; 17.91]
2050	**17.98** [16.98 ; 18.82]

Table 10.5.6: Single premiums calculated with the model with transitory jump effects and $Y \sim \mathcal{E}\mathrm{xp}\,(\lambda)$. Single premiums for the year 2020 are calculated using mortality rates observed during the year.

10.6 Appendix F.

Despite the fact that we do not have at our disposal the number of deaths and the risk exposures for the year 2020 for the Dutch population, we can still propose an estimation for these two tables. During the pandemic, the HMD team decided to provide a new data resource: **Short-term Mortality Fluctuations (STMF) data series**. These data series contain weekly death counts for different countries and time periods sorted by age group ($0 \to 14$; $15 \to 64$; $65 \to 74$; $75 \to 84$; 85+).

The STMF data series contains the number of weekly deaths for the year 2020 for the Dutch population. However, the risk exposures need to be estimated using data from previous years. Indeed, The risk exposures tend to have a predictable and regular trend over the last few years. If we want to find the ETR_x (i.e. risk exposures) of 2020 based on the previous ETR_x, an interesting thing to look at is the evolution of the ratio :

$$\frac{ETR_{x-1,t-1}}{ETR_{x,t}}$$

for a particular age x and year t.
If we do this for several t, we can compute the average of this ratio. We limit ourselves by calculating this ratio for the last 5 years (2015, 2016, 2017, 2018, 2019). The idea behind this is that the age is the variable which explains the most the evolution of a cohort from one year to another.

Let us take an example :
If we want to know the risk exposure of 2020 for the age 40, we need to look at this ratio for a few years earlier :

$$\frac{ETR_{39,2018}}{ETR_{40,2019}} \; ; \; \frac{ETR_{39,2017}}{ETR_{40,2018}} \; ; \; \frac{ETR_{39,2016}}{ETR_{40,2017}} \; ; \; \frac{ETR_{39,2015}}{ETR_{40,2016}}$$

We can take the mean of these ratios and call it "mean ratio_{40} ". With the following formula, we can give an estimation of the ETR_{40} for the year 2020 :

$$ETR_{40,2020} = \frac{ETR_{39,2019}}{\text{mean ratio}_{40}}.$$

Concerning the number of deaths, for reasons of accuracy, we must distribute the number of deaths for the year 2020 by age and not by age group. To do this, we distribute the number of deaths on a pro rata basis based on the contribution that each age has on the total number of deaths.

Let us take the age group 75-84 as an example and assume that 25,000 deaths were observed in this age group in 2020. We need to distribute this number of deaths over the 10 ages that make up this interval. To do this, we first fit a Lee-Carter model to the

period 1980 $\rightarrow$ 2019 and then project it forward one year to obtain a theoretical μ_x for 2020. Taking the ETR_x estimate for the year 2020 that we obtained with the method above and we can find the theoretical distribution of deaths for 2020 :

$$D_{x,2020}(\text{theoretical}) = \mu_{x,2020}(\text{theoretical}) \times ETR_{x,2020}.$$

We can then find the contribution that each age has on the number of deaths. For instance, if there is a total of 10 000 theoretical number of deaths over the 75 $\rightarrow$ 84 age group and that there is a total of 1 000 theoretical number of deaths for the age 75. Then the contribution of the age 75 is simply $1\,000/10\,000 = 0.1$.

Now, if we use the number of deaths observed for this age group (i.e. 25 000 for this example), we simply multiply this number by the contribution found above. In the end, we get our distribution of deaths per age for the year 2020. The estimate number of deaths and risk exposures for the Dutch population can be found in Figure 10.6.1.

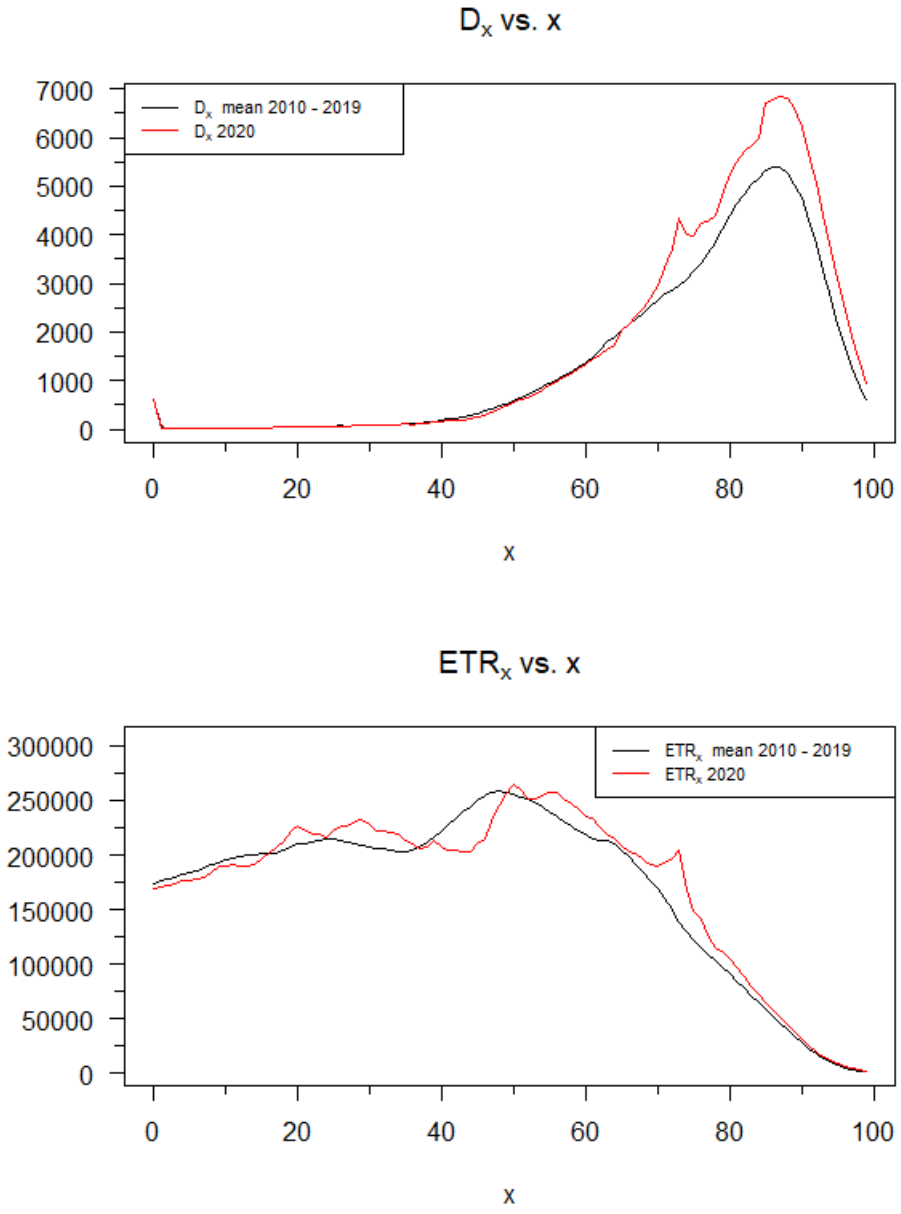

Figure 10.6.1: Number of deaths and risk exposure for the Dutch population. In red the estimation for the year 2020 and in black the average observed for the period 2010 $\rightarrow$ 2019.

10.7 Appendix G.

Projection without jump effects.

Time series: K_t

Time period	μ	σ
$1980 \rightarrow 2019$	-2.0338	1.9128
$1980 \rightarrow 2020$	-1.8670	2.1307

Time period	AIC	BIC
$1980 \rightarrow 2019$	165.26	168.59
$1980 \rightarrow 2020$	178.02	181.40

Table 10.7.1: Optimal parameters, AIC and BIC for K_t.

Time series: $\kappa_t(i)$

Time period	σ
$1980 \rightarrow 2019$	0.5015
$1980 \rightarrow 2020$	0.5155

Time period	AIC	BIC
$1980 \rightarrow 2019$	58.85	60.51
$1980 \rightarrow 2020$	62.51	64.20

Table 10.7.2: Optimal parameters, AIC and BIC for $\kappa_t(i)$ obtained with the RW projection method.

Time series: $\kappa_t(i)$

Time period	c_0	c_1	σ^*
$1980 \rightarrow 2019$	0.0078	0.6964	0.4651
$1980 \rightarrow 2020$	0.0111	0.7104	0.4822

Time period	AIC	BIC
$1980 \rightarrow 2019$	58.28	63.34
$1980 \rightarrow 2020$	62.53	67.67

Table 10.7.3: Optimal parameters, AIC and BIC for $\kappa_t(i)$ obtianed with the AR(1) projection method.

Projection with jump effects.

Calibration time period: 1980 → 2019

Projection model	AIC	BIC
PJ $Y \sim \mathcal{N}(m, s^2)$	169.31	177.63
PJ $Y \sim \mathcal{E}\text{xp}(\lambda)$	169.26	175.92
TJ $Y \sim \mathcal{N}(m, s^2)$	170.15	178.47
TJ $Y \sim \mathcal{E}\text{xp}(\lambda)$	170.02	176.68

Calibration time period: 1980 → 2020

Projection model	AIC	BIC
PJ $Y \sim \mathcal{N}(m, s^2)$	182.67	191.11
PJ $Y \sim \mathcal{E}\text{xp}(\lambda)$	181.68	188.44
TJ $Y \sim \mathcal{N}(m, s^2)$	183.49	191.93
TJ $Y \sim \mathcal{E}\text{xp}(\lambda)$	182.45	189.21

Table 10.7.4: AIC and BIC for the time series K_t with different projection model. PJ stands for projection model with permanent jump effects and TJ stands for projection model with transitory jump effects.

Calibration time period: 1980 → 2019

Projection model	AIC	BIC
PJ $Y \sim \mathcal{N}(m, s^2)$	64.73	71.39
PJ $Y \sim \mathcal{E}\text{xp}(\lambda)$	62.84	67.83
TJ $Y \sim \mathcal{N}(m, s^2)$	65.60	72.26
TJ $Y \sim \mathcal{E}\text{xp}(\lambda)$	63.63	68.62

Calibration time period: 1980 → 2020

Projection model	AIC	BIC
PJ $Y \sim \mathcal{N}(m, s^2)$	68.42	75.18
PJ $Y \sim \mathcal{E}\text{xp}(\lambda)$	66.50	71.57
TJ $Y \sim \mathcal{N}(m, s^2)$	69.28	76.04
TJ $Y \sim \mathcal{E}\text{xp}(\lambda)$	67.30	72.37

Table 10.7.5: AIC and BIC for the time series $\kappa_t(i)$ with different projection method with jump effects. PJ stands for projection model with permanent jump effects and TJ stands for projection model with transitory jump effects.

Bibliography

[1] Brouhns N, Denuit M, Vermunt J (2002). “A Poisson Log-Bilinear Regression Approach to the Construction of Projected Lifetables.” Insurance: Mathematics and Economics, 31(3), 373–393.

[2] Cairns AJG, Blake D, Dowd K (2006). “A Two-Factor Model for Stochastic Mortality with Parameter Uncertainty: Theory and Calibration.” Journal of Risk and Insurance, 73(4), 687–718.

[3] Chen H, Cox S (2009). "Modeling Mortality With Jumps: Applications to Mortality Securitization." Journal of Risk Insurance, 76, 727-751.

[4] Cox, Samuel and Lin, Yijia and Wang, Shaun, (2006). "Multivariate Exponential Tilting and Pricing Implications for Mortality Securitization." Journal of Risk and Insurance, 73(4): 719- 736.

[5] Currie ID (2016). “On Fitting Generalized Linear and non-linear Models of Mortality.” Scandinavian Actuarial Journal, (4), 356–383.

[6] Haberman S, Renshaw A (2011). “A Comparative Study of Parametric Mortality Projection Models.” Insurance: Mathematics and Economics, 48(1), 35–55.

[7] Lee RD, Carter LR (1992). “Modeling and Forecasting U.S. Mortality.” Journal of the American Statistical Association, 87(419), 659–671.

[8] Li N, Lee R (2005). “Coherent Mortality Forecasts for a Group of Populations: An Extension of the Lee-Carter Method.” Demography, 42(3), 575–594.

[9] Turner H, Firth D (2020). Generalized Nonlinear Models in R: An Overview of the gnm Package. R package version 1.1-1, URL `http://CRAN.R-project.org/package=gnm`.

[10] Villegas AM, Kaishev VK and Millossovich P (2018). “StMoMo: An R Package for Stochastic Mortality Modeling.” Journal of Statistical Software, 84(3), 1–38, URL `https://CRAN.R-project.org/package=StMoMo`.